Thesis Title

Institution Name

Author Name

Day Month Year

Notation

test

Chapter 1

Introduction

In particle physics we are concerned about small objects and their interactions. Since the 1970 the dynamics of elemental particles are best described by the Standard Model (SM).

The SM contains two groups of fermionic, spin 1/2 particles. The former group, the leptons consist of: the electron (e), the muon (μ), the tau (τ) and their corresponding neutrinos ν_e, ν_μ and ν_τ. The latter group, the quarks contain: u, d (up and down, the so called light quarks), s (strange), c (charm), b (bottom or beauty) and t (top or truth). The SM furthermore differentiates between three fundamental forces (and its carriers): the electromagnetic (γ photon), weak (Z-or W-Boson) and strong (g gluon) interactions. The before mentioned Leptons solely interact through the electromagnetic and the weak force (also referred to as electroweak interaction), whereas the quarks additionally interact through the strong force. A short summary of the taxonomy of the SM can be seen in fig. 1.1

All of the particles and forces given in the SM are described by a Lagrangian containing 19 parameters. The parameters are represented by ten masses, four CKM-matrix parameters, the QCD-vacuum angle, the Higgs-vacuum expectation value and three gauge coupling constants. Every single parameter has to be fitted from experimental data. Highly accurate values with low errors are crucial for theoretical calculated predictions. One of the major error inputs of every theoretical output are uncertainties in these parameters. In this work we will focus on one of the parameters, namely the strong coupling α_s, which forms part of the theory of *quantum chromodynamics* (QCD).

As the name suggest[1] QCD is characterized by the color charge. Every quark has next to its type one of the three colors blue, red or green. The color force is mediated through eight gluons, which each being bi-colored[2], interact with quarks and each other. The strength of the strong force is given by the coupling constant α_s. The strong coupling depends on the renormalization scale μ, which is often chosen in a way that the coupling constant $\alpha_s(q)$ depends on the

[1] Chromo is the Greek word for color.

[2] Each gluon carries a color and an anti-color.

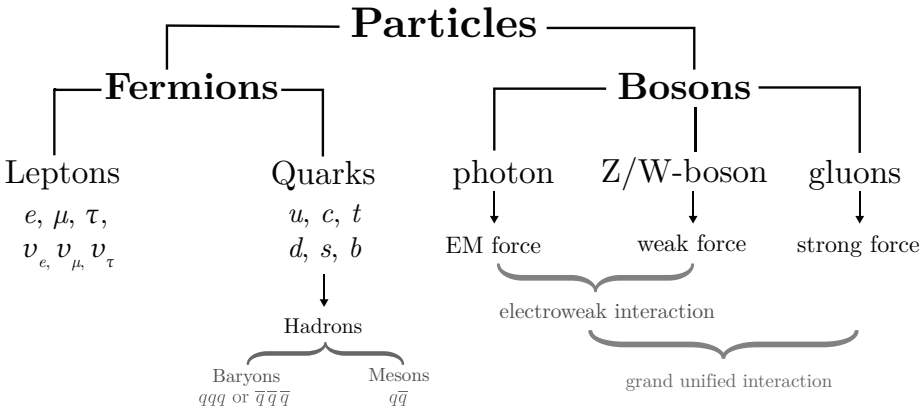

Figure 1.1: Taxonomy of the Standard Model.

energy q^2. Thus the coupling varies with energy with an exceptional property: it increases for low energies[3]. This is exclusive for QCD and has two main implications.

The first one states, that for low energies the coupling is too strong for isolate quarks to exist. Until now we have not been able to observe an isolated quark and all experiments can only measure quark compositions. These bound states are called *hadrons* and consist of two or three quarks [4], which are referred to as mesons[5] or baryons [6] respectively. This phenomenon, of quarks sticking together as hadrons is referred to as *confinement*. As the fundamental degrees of freedom of QCD are given by quarks and gluons, but the observed particles are hadrons we need to introduce the assumption of *quark-hadron duality* to match the theory to the experiment. This means that a physical quantity should be similarly describable in the hadronic picture or quark-gluon picture and that both descriptions are equivalent. As we will see in our work quark-hadron duality is violated for low energies. These so-called *duality violations* have an impact on our strong coupling determinations and can be dealt with either suppression or the inclusion of a model [**Pich2006**, 9]. Throughout this work we will favor and argument for the former approach.

The second implication concerns *perturbation theory* (PT). The lower the energies we deal with, the higher the value of the strong coupling and the contributions of *non-perturbative* (NP) effects. Currently there are three solutions to deal with NP effects:

[3] In contrast to the electromagnetic force, where $\alpha(q^2)$ decreases!
[4] There exist also so-called *Exotic hadrons*, which have more than three valence quarks.
[5] Composite of a quark and an anti-quark.
[6] Composite of three quarks or three anti-quarks.

- ***Chiral Perturbation Theory*** (ChPT): Introduced by Weinberg [37] in the late seventies. ChPT is an effective field theory constructed with a Lagrangian symmetric under chiral transformation in the limit of massless quarks. It's limitations are based in the chiral symmetry, which is only a good approximation for the light quarks u, d and in some cases s.

- ***Lattice QCD*** (LQCD): Is the numerical approach to the strong force. Based on the Wilson Loops [38] we treat QCD on a finite lattice instead of working with continuous fields. LQCD has already many applications but is limited due to its computational expensive calculations.

- ***QCD Sum Rules*** (QCDSR): Was also introduced in the late seventies by Shifman, Vainstein and Zakharov [33, 32]. It relates the observed hadronic picture to quark-gluon parameters through a dispersion relation and the use of the *Operator Product Expansion* (OPE), which treats NP effect through the definition of vacuum expectation values, the so-called *QCD condensates*. It is a precise method for extracting the strong coupling α_s at low energies, although limited to the unknown higher order contributions of the OPE.

In this work we focus on the determination of the strong coupling α_s within the framework of QCD Sum Rules for τ-decays which has been exploited in the beginning of the nineties by Braaten, Narison and Pich [6]. Within this setup we can measure $\alpha_s(m_\tau^2)$ at the m_τ scale. As the strong coupling gets smaller at higher energies, so do the errors. Thus if we obtain the strong coupling at a low scale we will obtain high precision values at the scale of the Z-boson mass m_Z, which is the standard scale to compare α_s values.

The QCDSR for the determination of α_s, from low energies, contain three major issues.

1. There are two different approaches to treat perturbative and non-perturbative contributions. In particular, there is a significant difference between results obtained using fixed-order (FOPT) or contour improved perturbation theory (CIPT), such that analyses based on CIPT generally arrive at about 7% larger values of $\alpha_s(m_{\tau^2})$ than those based on FOPT [35]. There have been a variety of analyses on the topic been performed [27, 8, 18] and we will favor the FOPT approach, but generously list our results for the CIPT framework.

2. There are several prescriptions to deal with the NP-contributions of higher order OPE condensates. Typically terms of higher dimension have been neglected, even if they knowingly contribute. In this work we will include every necessary OPE term.

3. Finally there are known DV leading to an ongoing discussion of the importance of contributions from DV. Currently there are two main approaches: Either we neglect them, arguing that they are sufficiently suppressed due

to *pinched weights* [28] or model DV with sinusoidal exponentially suppressed function [9, 3, 5] introducing extra fitting parameters. We will argue for the former method, implementing pinched weights that sufficiently suppress DV contributions such as having only a negligible effect on our analysis.

In the first chapter of this work we want to summarize the necessary theoretical background for working with the QCDSR. Starting with the basics of QCD we want to motivate the *renormalization group equation* (RGE), which is responsible for the running of the strong coupling. We then continue with the some aspects of the two-point function and its usage in the dispersion relation, which connects the hadronic picture with the quark-gluon picture. $\cdots$

Chapter 2

Theoretical Background

2.1 Quantumchromodynamics

QCD gives a complete description of *quarks* and *gluons*. It is born out of the very successful theory of *quantum electrodynamics* (QED), but has some major differences. QED has two well known constituent fields the fermion and the photon. It is also a so called *abelian* theory, meaning that two consecutive rotations commute $AB = BA$. Due to the abelian nature of the QED gauge group $U(1)$ only fermions carry gauge charge. Photons do not carry charge. In contrast QCD takes quarks[1] and gluons as fields. Additionally QCD is ruled by a *non-abelian* gauge symmetry of $SU(3)$. Thus the group operation of QCD in general do not commute, which leads to gluons carrying charge! This charge is called *color-charge*. The theory requieres three colors and describes interactions between a quark of a color with a quark of another color via gluons. Contrary to QED the force carrier, the gluons, interact with themselve, because they carry color charge. The corresponding Feynman diagrams can be seen in fig. 2.1.

[1] Quarks are a subset to the fermions.

Flavour	Mass
u	3.48(24) MeV
d	6.80(29) MeV
s	130.0(18) MeV
c	1.523(18) GeV
b	6.936(57) GeV
t	173.0(40) GeV

Table 2.1: List of Quarks and their masses. The masses of the up, down, strange, charm and bottom quark are the renormalization group invariant (RGI) quark masses and are quoted in the four-flavour theory ($N_f = 2 + 1$) at the scale $\mu = 2\,\text{GeV}$ in the $\overline{MS}$ scheme and are taken from the *Flavour Lattice Averaging Group* [**FLAG2019**]. The mass of the top quark is not disucess in [**FLAG2019**] and has been taken from [35] from direct observations of top events.

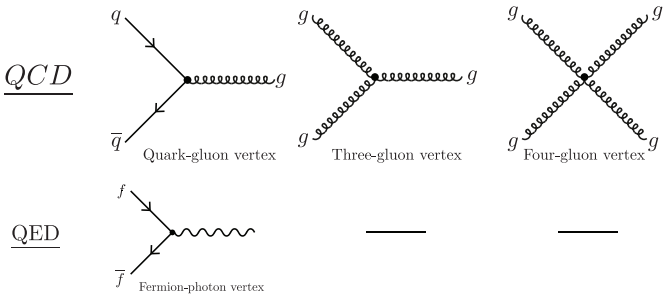

Figure 2.1: Feynman diagrams of the strong interactions with corresponding electromagnetic diagrams. We see that the gluons carry color-charge and thus couple to other gluons, which is not the case for the photons.

The theory of QCD can be summarized with its *Lagrange density*[19]:

$$\mathcal{L}_{QCD}(x) = -\frac{1}{4}G^a_{\mu\nu}(x)G^{\mu\nu a}(x) + \sum_A \left[\frac{i}{2}\bar{q}^A(x)\gamma^\mu \overleftrightarrow{D}_\mu q^A(x) - m_A\bar{q}^A(x)a^A(x)\right], \tag{2.1}$$

where $q^A(x)$ represents the quark fields and $G^a_{\mu\nu}$ being the *gluon field strength tensor* given by:

$$G^a_{\mu\nu}(x) \equiv \partial_\mu B^a_\nu(x) - \partial^a_\nu(x) + gf^{abc}B^b_\mu(x)B^c_\nu(x), \tag{2.2}$$

where B^a_μ are the *gluon fields*, given in the *adjoint representation* of the SU(3) gauge group with f^{abc} as *structure constants*. Furthermore we have used $A, B, \ldots = 0, \ldots 5$ as flavour indices, $a, b, \ldots = 0, \ldots, 8$ as color indices and $\mu, \nu, \ldots = 0, \ldots 3$ as lorentz indices.

2.1.1 Renormalisation Group

The perurbations of the QCD Lagrangian 2.1 lead to divergencies, which have to be *renormalized*. There are different aproaches to 'make' these divergencies finite. The most popular one is **dimensional regularisation**.

In *dimensional regularisation* we expand the four space-time dimensions to arbitrary dimensions. Consequently the in QCD calculations appearing *Feyman integrals* have to be continued to D-dimensions like

$$\mu^{2\epsilon}\int \frac{\mathrm{d}^D p}{(2\pi)^D}\frac{1}{[p^2 - m^2 + i0][(q-p)^2 = m^2 + i0]}, \tag{2.3}$$

where we introduced the scale parameter μ to account for the extra dimensions and conserve the mass dimension of the non continued integral.

In addition *physical quantities*[2] cannot depend on the renormalisation scale μ. Thus the derivative by μ of a general *physical quantity* $R(q, a_s, m)$ that

[2]Observables that can be measured.

depends on the external momentum q, the renormalised coupling $a_s \equiv \alpha_s/\pi$ and the renormalized quark mass m has to yield zero

$$\mu \frac{\mathrm{d}}{\mathrm{d}\mu} R(q, a_s, m) = \left[\mu \frac{\partial}{\partial \mu} + \mu \frac{\mathrm{d}a_s}{\mathrm{d}\mu} \frac{\partial}{\partial m} + \mu \frac{\mathrm{d}m}{\mathrm{d}\mu} \frac{\partial}{\partial m} \right] R(q, a_s, m) = 0. \tag{2.4}$$

eq. (2.4) is referred to as **renormalization group equation** and is the basis for defining the *renormalisation group functions*:

$$\beta(a_s) \equiv -\mu \frac{\mathrm{d}a_s}{\mathrm{d}\mu} = \beta_1 a_s^2 + \beta_2 a_s^3 + \ldots \qquad \beta - \text{function} \tag{2.5}$$

$$\gamma(a_s) \equiv -\frac{\mu}{m} \frac{\mathrm{d}m}{\mathrm{d}\mu} = \gamma_1 a_s + \gamma_2 a_s^2 + \ldots \qquad \text{anomalous mass dimension.} \tag{2.6}$$

Running gauge coupling

The β-function and the anomalous mass dimension are responsible for the running of the strong coupling and the running of the quark mass respektively. In this section we will shortly review the β-function and its implications on the strong coupling, whereas in the following section we will discuss the anomalous-mass dimension.

Regarding the β-function we notice, that $a_s(\mu)$ is not a constant, but *runs* by varying its scale μ. Lets observe the running of the strong coupling constant by integrating the β-function

$$\int_{a_s(\mu_1)}^{a_s(\mu_2)} \frac{\mathrm{d}a_s}{\beta(a_s)} = -\int_{\mu_1}^{\mu_2} \frac{\mathrm{d}\mu}{\mu} = \log \frac{\mu_1}{\mu_2}. \tag{2.7}$$

To analytically evaluate the above integral we can approximate the β-function to first order, with the known coefficient

$$\beta_1 = \frac{1}{6}(11 N_c - 2 N_f), \tag{2.8}$$

yielding

$$a_s(\mu_2) = \frac{a_s(\mu_1)}{\left(1 - a_s(\mu_1)\beta_1 \log \frac{\mu_1}{\mu_2}\right)}. \tag{2.9}$$

As we have three colours $N_c = 3$ and six flavours $N_f = 6$ the first β-function 2.5 is positive. Thus for $\mu_2 > \mu_1$ $a_s(\mu_2)$ decreases logarithmically and vanishes for $\mu_2 \to \infty$. This behaviour is known as *asymptotic freedom*. The coefficients of the β-function are currently known up to the 5th order and listed in the appendix 5.1.

As QCD we have three colors and six flavours the beta function carries a negative sign (see eq. (2.8)). This implies that the strength of the coupling is **decreasing** for increasing energies. In QED we have a beta-function with a positive sign and thus its coupling strength increases with energy. This behaviour of QCD leads to *confinement* and *asymptotic freedom*.

Color confinement, or simply confinement, means that color charged quarks cannot be isolated. They always appear in composite hadrons. Until today

no quark has been measured as single particle. There is no analytic proof of confinement, but until today no single quark has been observed. It is qualitativly explained with the gluon field carrying color charge. These gluons form so-called *flux-tubes* between quarks, which cause a constant strong force between particles regardless of their separation. Consequently the energy needed to separate quarks is proportional to the distance between them and at some point there is enough energy to favour the creation of a new quark pair. Thus before separating two quarks we create a two new quarks and we will probably never be able to observe an isolated quark.

For high energies, or very close quarks, the QCD coupling becomes weak and the quarks and gluons are essentially free. This phenomen is refered to as asymptotic freedom.

Running quark mass

Not only the coupling but also the masses carry an energy dependencies, which is governed by the *anomalou mass dimension* $\gamma(a_s)$.

The properties of the running quark mass can be derived similar to the gauge coupling. Starting from integrating the *anomalous mass dimension* 2.6

$$\log \frac{m(\mu_2)}{m(\mu_1)} = \int_{a_s(\mu_1)}^{a_s(\mu_2)} \mathrm{d}a_s \frac{\gamma(a_s)}{\beta(a_s)} \tag{2.10}$$

we can approximate the *anomalous mass dimension* to first order and solve the integral analytically [31]

$$m(\mu_2) = m(\mu_1) \left(\frac{a(\mu_2)}{a(\mu_1)} \right)^{\frac{\gamma_1}{\beta_1}} \left(1 + \mathcal{O}(\beta_2, \gamma_2) \right). \tag{2.11}$$

As β_1 and γ_1 (see 5.2) are positive the quark mass decreases with increasing μ. The general relation between different scales is given by

$$m(\mu_2) = m(\mu_1) \exp \left(\int_{a_s(\mu_1)}^{a_s(\mu_2)} \mathrm{d}a_s \frac{\gamma(a_s)}{\beta(a_s)} \right) \tag{2.12}$$

and can be solved numerically to run the quark mass to the needed scale μ_2.

QCD in general has a precision problem caused by uncertainties and largness of the strong coupling constant α_s. The fine-structure constant (the coupling constant of QED) is known to eleven digits, whereas the strong coupling is only known to about four. Furthermore for low energies the strong coupling constant is much larger than the fine-structure constant. E.g. at the Z-mass, the standard mass to compare the strong coupling, we have an α_s of 0.11, whereas the fine structure constant would be around 0.007. Consequently to use PT we have to calculate our results to much heigher orders, including tens of thousends of Feynman diagrams, in QCD to achieve a precision equal to QED. For even lower energies, around 1 GeV, the strong coupling reaches a critical value of ≈ 0.5 leading to a break down of PT.

In this work we try to achieve a higher precision in the value of α_s. Our method to measure the strong coupling is called **QCD sum rules**, which by itself is based on a concept called the *two-point function* for which we will devote the following section.

2.1.2 Two-Point function

The vacuum expectation value of the product of the conserved noether current $J_\mu(x)$ at different space-times points x and y is known as the **two-point function** (or simply **correlator**)

$$\Pi_{\mu\nu}(q^2) = \langle 0|J_\mu(x)J_\nu(y)|0\rangle, \tag{2.13}$$

where the noether current is given by

$$J_\mu(x) = \overline{q}\,(x)\Gamma q(y) \tag{2.14}$$

, where Γ stands for one of the dirac matrices $\Gamma \in \{1, i\gamma_5, \gamma_\mu, \gamma_\mu\gamma_5\}$, specifying the quantum number of the current (S: *scalar*, P: *pseudo-Scalar*, V: *vectorial*, A: *axial-vectorial*, respectively).

The correlator tensor $\Pi_{\mu\nu}(q^2)$ can be lorentz decomposed to a scalar function $\Pi(q^2)$. There are only two possible terms that can reproduce the second order tensor $q_\mu q_\nu$ and $q^2 g_{\mu\nu}$. The sum of both multiplied with two arbitrary functions $A(q^2)$ and $B(q^2)$ yields

$$\Pi_{\mu\nu}(q^2) = q_\mu q_\nu A(q^2) + q^2 g_{\mu\nu} B(q^2). \tag{2.15}$$

By making use of the **Ward-identity** [26]

$$q^\mu \Pi_{\mu\nu}(q^2) = q^\nu \Pi_{\mu\nu} = 0 \tag{2.16}$$

we can demonstrate, that the two arbitrary functions are related

$$\begin{aligned} q^\mu q^\nu \Pi_{\mu\nu} = q^4 A(q^2) + q^4 B(q^2) = 0 \\ \implies A(q^2) = -B(q^2). \end{aligned} \tag{2.17}$$

Thus redefining $A(q^2) \equiv \Pi(q^2)$ we expressed the correlator as a scalar function

$$\Pi_{\mu\nu}(q^2) = (q_\mu q_\nu - q^2 g_{\mu\nu})\Pi(q^2). \tag{2.18}$$

The scalar QCD two point function can then be related to the spectrum of hadronic states. The correlator is then related to an integral over the **spectral function** $\rho(s)$ via the *Källén-Lehmann spectral representation* [21, 24], which is known since the early fities

$$\Pi(q^2) = \int_0^\infty \mathrm{d}s \frac{\rho(s)}{s - q^2 - i\epsilon}. \tag{2.19}$$

Equation 2.19 is refered to as **dispersion relation** analogous to similar relations which arise for example in electrodynamics and defines the **spectral function** (a derivation can be found in [29])

$$\rho(s) = \frac{1}{\pi} \operatorname{Im} \Pi(s). \tag{2.20}$$

Until know we connected theoretical correlators with the measurable hadronic spectrum. Nevertheless the analytic properties of the correlators have to be discussed as the function has discontinuities.

The main contribution from the spectral function given in eq. (2.19) are the hadronic final states

$$2\pi\rho(m^2) = \sum_n \langle 0|J_\mu(x)|n\rangle\langle n|J_\nu(y)\rangle(2\pi^2)^4\delta^{(4)}(p-p_n), \tag{2.21}$$

which lead to a series of continuous poles on the positive real axis for the two-point function, see Fig. 2.2. These discontinuities can be tackled with *Cauchy's*

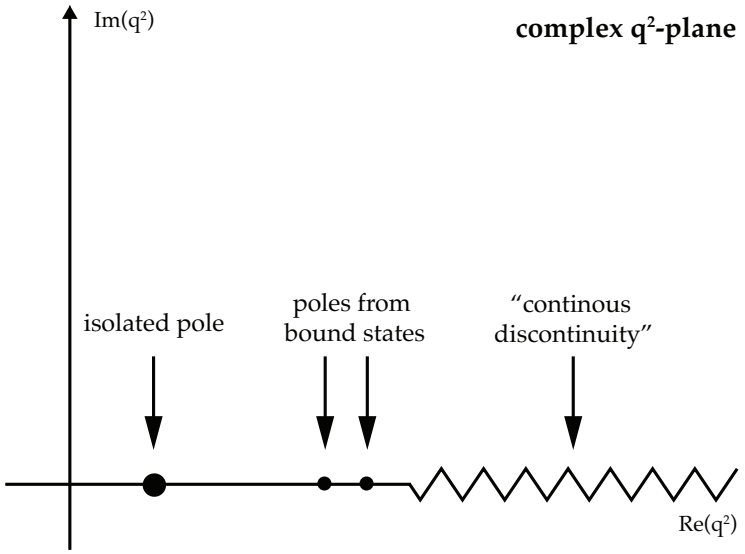

Figure 2.2: Analytic structure in the complex q^2-plane of the Fourier transform of the two-point function. The hadronic final states are responsible for poles appearing on the real-axis. The one-particle states contribute as isolated pole and the multi-particle states contribute as bound-states poles or a continues "discontinuity cut" [26].

theorem, which we will apply in **??**.

Until now we exclusively dealt with the perturbative (PT) part of the theory, but QCD is known to have not negligible non-perturbative (NPT) contributions. Thus before continuing with the *Sum Rules* we need a final ingredient the operator product expansion, which implements NPT cotributions to our theory.

2.1.3 Operator Product Expansion

The **Operator Product Expansion** (OPE) was introduced by Wilson in 1969 [39]. The expansion states that non-local operators can be rewritten into a sum of composite local operators and their corresponding coefficients:

$$\lim_{x\to y} \mathcal{O}_1(x)\mathcal{O}_2(y) = \sum_n C_n(x-y)\mathcal{O}_n(x), \tag{2.22}$$

where $C_n(x-y)$ are the so-called *Wilson-coefficients*.

The OPE lets us separate *short-distance* from *long-distance* effects. In perturbation theory (PT) we can only amount for *short-distances*, which are equal to hight energies, where the strong-coupling α_s is small. Consequently the OPE decodes the long-distance effects in the higher dimensionsional operators.

The form of the composite operators are dictated by Gauge- and Lorentz symmetry. Thus we can only make use of operators of even dimension. The operators up to dimension six are given by [25]

$$\begin{array}{ll} \text{Dimension 0:} & \not\Vdash \\ \text{Dimension 4:} & :m_i\overline{q}\,q: \\ & :G_a^{\mu\nu}(x)G^a_{\mu\nu}(x): \\ \text{Dimension 6:} & :\overline{q}\,\Gamma q\overline{q}\,\Gamma q: \\ & :\overline{q}\,\Gamma\frac{\lambda^a}{2}q_\beta(x)\overline{q}\,\Gamma\frac{\lambda^a}{2}q: \\ & :m_i\overline{q}\,\frac{\lambda^a}{2}\sigma_{\mu\nu}qG_a^{\mu\nu}: \\ & :f_{abc}G_a^{\mu\nu}G_b^{\nu\delta}G_c^{\delta\mu}:, \end{array} \tag{2.23}$$

where Γ stands for one of the dirac matrices $\Gamma \in \{1, i\gamma_5, \gamma^\mu, \gamma^\mu\gamma_5\}$, specifying the quantum number of the current (S, P, A, respectively). As all the operators appear normal ordered they vanish by definition in PT. Consequently they appear as **Condensates** in Non-perturbative (NPT) QCD like quark-condensate $\langle\overline{q}\,q\rangle$ or the gluon-condensate $\langle aGG\rangle$ (both of dimension four). These non-vanishing condensats characterize the QCD-vacuum.

As we work with dimensionless functions (e.g. Π) in Sum Rules, the r.h.s. of **??** has to be dimensionless. Consequently the Wilson-coefficients have to cancel the dimension of the operator with their inverse mass dimension. To account for the dimensions we can make the inverse momenta explicit

$$\Pi^{OPE}_{V/A}(s) = \sum_{D=0,2,4\ldots} \frac{c^{(D)}\langle\mathcal{O}^{(D)}(x)\rangle}{-s^{D/2}}, \tag{2.24}$$

where we used $C^{(D)} = c/(-s)^{D/2}$ with D being the dimension. Consequently the OPE should converge with increasing dimension for suficienty large momenta s.

Let's show how the OPE contributions are calculated with a the "standard example" (following [**Pascual1986**]), where we compute the perturbative and quark-condensate Wilson-coefficients for the ρ-meson. For the ρ-meson, which is composed of u and d quarks, the current of eq. (2.13) takes the following form

$$j^\mu(x) = \frac{1}{2}\left(:[\overline{u}\,\gamma^\mu u](x) - \overline{d}\,\gamma^\mu d](x)\right). \tag{2.25}$$

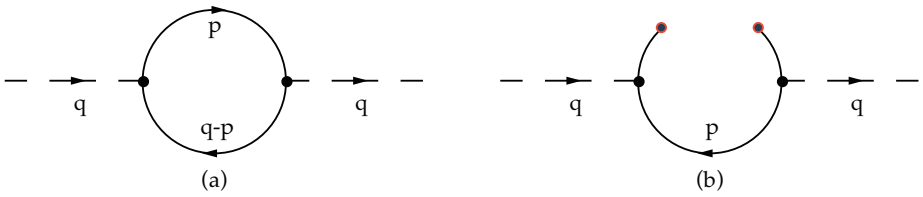

Figure 2.3: Feynman diagrams of the perturbative (a) and the quark-condensate (b) contribution. The upper part of the right diagram is not wick-contracted and responsible for the condensate.

In fig. 2.3 we draw the Feynman-diagram, from which we can take the uncontracted mathematical expression for the scalar correlator

$$\begin{aligned}\Pi(q^2) = -\frac{i}{4q^2(D-1)} \int \mathrm{d}^D x e^{iqx} \langle \Omega | T\{ : \overline{u}(x)\gamma^\mu u(x) - \overline{d}(x)\gamma^{mu} d(x) : \\ \times : \overline{u}(0\gamma_\mu u(0) - \overline{d}(0)\gamma_\mu d(0) : \}\rangle.\end{aligned} \tag{2.26}$$

Using Wick's theorem we can contract all of the fields and calculate the first term of the OPE (⊮), which represents the perturbative contribution of the OPE (⊮)

$$\begin{aligned}\Pi(q^2) &= \frac{i}{4q^2(D-1)} (\gamma^\mu)_{ij}(\gamma_\mu)_{kl} \int \mathrm{d}^D x e^{iqx} \\ &\times \quad \left[\overbrace{u_{j\alpha}(x)\overline{u}}_{k\beta}(0) \cdot \overbrace{u_{l\beta}(0)\overline{u}}_{i\alpha}(x) + (u \to d) \right] \\ &= \frac{3}{8\pi^2} \left[\frac{5}{3} - \log\left(-\frac{q^2}{\nu^2} \right) \right].\end{aligned} \tag{2.27}$$

To calculate the higher dimensional contributions of the OPE we use the same techniques as before, but leave some of the fields uncontracted. For the quark-condensate, which we want to derive for tree-level, we leave two fields uncontracted

$$\begin{aligned}\Pi(q^2) = \frac{i}{4q^2(D-1)} (\gamma^\mu)_{ij}(\gamma_\mu)_{kl} \int \mathrm{d}^D x e^{iqx} \Big[\\ + \overbrace{u_{j\alpha}(x)\overline{u}}_{k\beta}(0) \cdot \langle \Omega | : \overline{u}_{i\alpha}(x) u_{l\beta}(0) : | \Omega \rangle \\ + \overbrace{u_{l\beta}(0)\overline{u}}_{i\alpha}(x) \cdot \langle \Omega | : \overline{u}_{k\beta}(0) u_{j\alpha}(x) : | \Omega \rangle + (u \to d) \Big].\end{aligned} \tag{2.28}$$

The non contracted fields can then be expanded in x

$$\begin{aligned}\langle \Omega | : \overline{q}(x) q(0) : | \Omega \rangle = \langle \Omega | : \overline{q}(0) q(0) : | \Omega \rangle \\ + \langle \Omega | : \left[\partial_\mu \overline{q}(0) \right] q(0) : | \Omega \rangle x^\mu + \dots\end{aligned} \tag{2.29}$$

and redefined to a more elegant notation

$$\langle \overline{q}\, q \rangle \equiv \langle \Omega | : \overline{q}\,(0) q(0) : | \Omega \rangle. \tag{2.30}$$

The finally result can be taken from [25] and yields

$$\Pi_{(\rho)}(q^2) = \frac{1}{2} \frac{1}{(-q^2)^2} \left[m_u \langle \overline{u}\, u + m_d \langle \overline{d}\, \rangle \right]. \tag{2.31}$$

The usage of the OPE and its validity is far from obvious. We are deriving the OPE from matching the Wilson-coefficients to Feynman-graph analyses. These Feynman-graphs are calculated perturbatively but the coefficients with dimension $D > 0$ correspond to NPT condensates!

Having gathered all of the necessary concepts we can close the gap between the theory and experiment in the last section of the introduction: QCD Sum Rules.

2.1.4 Sum Rules

To relate the measurable hadronic final states of a QCD process (e.g. τ-decays into Hadrons) to a theoretical calculable **QCD sum rules** have been empliyed by Shifman in the late sevent [33].

The sum rules are a combination of the two-point function and its analyticity, the OPE, a dispersion relation, the optical theorem and quark hadron duality.

The previously introduced two-point function eq. (2.13) is generally descriped by the OPE to account for NPT effects.

$$\Pi(q^2) = \Pi^{OPE}(q^2). \tag{2.32}$$

Furthermore it is related to the theoretical spectral function $\rho(s)$ via a dispersion relation **??**eq:dispersionRelation). Using QCD we are computing interactions based on quarks and gluons, but due to confinement, we are only able to observe Hadrons. Consequently to connect the theory to the experiment we have to assume **quark-hadron duality**[3], which implies that physical quantities can be described equally good in the hadronic or in the quark-gluon picture. Thus we can rewrite the dispersion relation eq. (2.19) as

$$\Pi_{th}^{OPE}(q^2) = \int_0^\infty \frac{\rho_{exp}(q^2)}{(s - q^2 - i\epsilon)}, \tag{2.33}$$

where we connected the theoretical correlator Π_{th} with the experimental measurable spectral function ρ_{exp}.

We have seen that the theoretical description of the correlator Π_{th} contains poles on the real axis, but the experimental data ρ_{exp} is solely accesible on the positive real axis. Thus we have to make use of Cauchy's theorem to access the

[3] Or simply duality.

theoretical values of the two-point function close to the postive real axis (see section 2.1.4) given by

$$\int_{\mathcal{C}} f(z)\,\mathrm{d}z = 0, \tag{2.34}$$

where $f(z)$ is an analytic function on a closed contour $\mathcal{C}$.

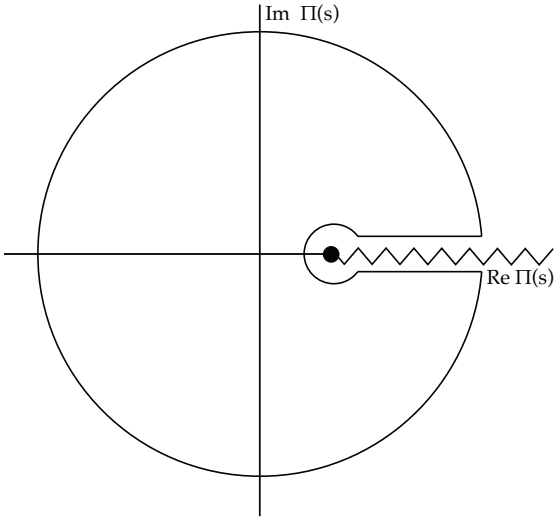

Figure 2.4: Analytical structure of $\Pi(s)$ with the used contour $\mathcal{C}$ for the final QCD Sum Rule expression eq. (2.35).

The final ingredient of the QCD sum rules is the *optical theorem*, relating experimental data with the imaginary part of the correlator (the spectral function $\rho(s)$).

In total, with the help Cauchy's theorem, the QCD sum rules can be sumed up in the following expression

$$\frac{1}{\pi}\int_0^\infty \frac{\rho_{exp}(t)}{t-s}\,\mathrm{d}t = \frac{1}{\pi}\oint_{\mathcal{C}} \frac{\mathrm{Im}\,\Pi_{OPE}(t)}{t-s}\,\mathrm{d}t, \tag{2.35}$$

where the l.h.s. is given by the experiment and the r.h.s. can be theoretically evaluated with by applying the OPE of the correlator $\Pi_{OPE}(s)$.

Chapter 3

τ decays into hadrons

The principal input to our QCD analysis are measurements of τ-decays, which represent an excellent tool to access low energy QCD.

The τ-particle is an elementary particle with negative electric charge and a spin of 1/2. Together with the lighter electron and muon it forms the *charged Leptons*[1]. Even though it is an elementary particle it decays via the *weak interaction* with a lifetime of $\tau_\tau = 2.9 \times 10^{-13}$ s and has a mass of 1776.86(12) MeV[35]. It is furthermore the only lepton massive enough to decay into Hadrons. The final states of a decay are limited by *conservation laws*. In case of a τ-decay they must conserve the electric charge (-1) and *invariant mass* of the system. Thus, as we can see from the corresponding Feynman diagram (see fig. 3.1)[2] the τ decays by the emission of a *W boson* and a tau-neutrino ν_τ into pairs of $(e^-, \bar{\nu}_e), (\mu^-, \bar{\nu}_\mu)$ or $(q, \bar{q})$.

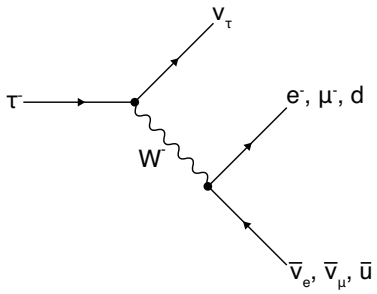

Figure 3.1: Feynman diagram of common decay of a τ-lepton into pairs of lepton-antineutrino or quark-antiquark by the emission of a *W boson*.

taken from tau decay adapt! We are foremost interested into the hadronic decay channels, meaning τ-decays that have quarks in their final states. Un-

[1] Leptons do not interact via the strong force.

[2] The τ-particle can also decay into strange quarks or charm quarks, but these decays are rather uncommon due to the heavy masses of s and c.

Name	Symbol	Quark content	Rest mass (MeV)
Pion	π^-	$\bar{u}d$	139.570 61(24) MeV
Pion	π^0	$(u\bar{u} - d\bar{d})/\sqrt{2}$	134.9770(5) MeV
Kaon	K^-	$\bar{u}s$	493.677(16) MeV
Kaon	K^0	$d\bar{s}$	497.611(13) MeV
Eta	η	$(u\bar{u} + d\bar{d} - 2s\bar{s})/\sqrt{6}$	547.862(17) MeV

Table 3.1: List of mesons produced by a τ-decay. Rare final states with branching Ratios smaller than 0.1 have been omitted. The list is taken from [14] with corresponding rest masses taken from [35].

fortunately the quarks have never been measured isolated, but appear always in combination of *mesons* and *baryons*. Due to its mass of $m_\tau \approx 1.8\,\text{GeV}$ the τ-particle decays into light mesons (pions-π, kaons-K, and eta-η, see table 3.1), which can be experimentally detected.

The hadronic $\tau - decay$ provides one of the most precise ways to determine the strong coupling [28] and can be calculated to high precision within the framework of QCD.

begin old The τ-lepton is the only lepton heavy enough to decay into Hadrons. It permits one of the most precise determinations of the strong coupling α_s. The inclusive τ-decay ratio

$$R_\tau = \frac{\Gamma(\tau \to \nu_\tau + \text{Hadrons})}{\Gamma(\tau \to \nu_\tau e^+ e^-)} \tag{3.1}$$

can be precisely calculated and is sensitive to α_s. Due to low the mass of the τ-lepton $m_\tau \approx 1.8\,\text{GeV}$ τ-decays are excellent for performing a low-energy QCD analysis. The theoretical expression of the hadronic τ-decay ratio was first derived by [36], using current algebra, a more recent derivation making use of the *optical theorem* can be taken from [31]. The inclusive ratio is then given by:

$$R_\tau(s) = 12\pi \int_0^{m_\tau} = \frac{\mathrm{d}s}{m_\tau^2}\left(1 - \frac{s}{m_\tau^2}\right)\left[\left(1 + 2\frac{s}{m_\tau^2}\right)\operatorname{Im}\Pi^{(T)}(s) + \operatorname{Im}\Pi^{(L)}(s)\right], \tag{3.2}$$

where $\operatorname{Im}\Pi$ is the two-point function (see section 2.1.2). In the case of τ-decays we only have to consider vector (V) and axial-vector contributions (A) of decays into up, down and strange quarks. Thus taking i, j as the flavour indices for the light quarks (u, d and s) we can express the correlator as

$$\Pi^{V/A}_{\mu\nu,ij}(s) \equiv i \int \mathrm{d}x\, e^{ipx} \langle\Omega|T\{J^{V/A}_{\mu,ij}(x) J^{V/A}_{\nu,ij}(0)^\dagger\}|\Omega\rangle, \tag{3.3}$$

with $|\Omega\rangle$ being the physical vacuum. The vector and axial-vector currents are then distinguished by the corresponding dirac-matrices ($\gamma_\mu$and$\gamma_\mu\gamma_5$) given by

$$J^V_{\mu,ij}(x) = \overline{q}_j(x)\gamma_\mu q_i(x) \quad \text{and} \quad J^A_{\mu,ij}(x) = \overline{q}_j(x)\gamma_\mu\gamma_5 q_i(x). \tag{3.4}$$

The two-point function can be decomposed into its vector and axial-vector contributions, but also into transversal and longitudinal components. We will give now both of these decompositions and relate them, which has some implications for a common used approximation: the **chiral limit**, where the quark masses are taken to 0 ($m_q \to 0$).

Starting with the decomposition into vector, axial-vector, scalar (S) and pseudo-scalar (P) components we can write [7, 20]

$$\begin{aligned}\Pi^{\mu\nu}(q^2) = (q^\mu q^\nu - q^2 g^{\mu\nu})\Pi^{V,A}(q^2) + \frac{g^{\mu\nu}}{q^2}(m_i \mp m_j)\Pi^{S,P}(q^2) \\ + g^{\mu\nu}\frac{(m_i \mp m_j)}{q^2}[\langle \overline{q}_i q_i\rangle \mp \langle \overline{q}_j q_j\rangle],\end{aligned} \tag{3.5}$$

which is composed of a vector $\Pi^{V,A}$ and scalar $\Pi^{S,P}$ part. The third term are corrections arising due to the physical vacuum $|\Omega\rangle$. The latter decomposition rewrites the correlator $\Pi^{\mu\nu}(q^2)$ into transversal and longitudinal components:

$$\Pi^{\mu\nu}(q^2) = (q^\mu q^\nu - g^{\mu\nu}q^2)\Pi^{(T)}(q^2) + q^\mu q^\nu \Pi^{(L)}(q^2). \tag{3.6}$$

With the two decompositions eq. (3.5) and eq. (3.6) we can now identify the longitudinal components of the correlator as being purely scalar, by multiplying eq. (3.5) by two four-momenta and making use of the Ward-idendity eq. (2.16) we can write

$$q_\mu q_\nu \Pi^{\mu\nu}(q^2) = (m_i \mp m_j)^2 \Pi^{S,P}(q^2) + (m_i \mp m_j)[\langle \overline{q}_i q_i\rangle \mp \langle \overline{q}_j q_j\rangle], \tag{3.7}$$

which then can be related to the longitudinal component of eq. (3.6) by comparisson of the two equations

$$q_\mu q_\nu \Pi^{\mu\nu}(q^2) = q^4 \Pi^{(L)}(q^2) = s^2 \Pi^{(L)}(s) \quad \text{with} \quad s \equiv q^2. \tag{3.8}$$

In a more eloquent way this can be expressed as

$$s^2 \Pi^{(L)}(s) = (m_i \mp m_j)^2 \Pi^{(S,P)}(s) + (m_i \mp m_j)[\langle \overline{q}_i q_i\rangle \mp \langle \overline{q}_j q_j\rangle], \tag{3.9}$$

where we can see, that all mass terms are related to the longitudinal component of the correlator. By defining a combination of the transversal and longitudinal correlator

$$\Pi^{(T+L)}(s) \equiv \Pi^{(T)}(s) + \Pi^{(L)}(s) \tag{3.10}$$

we can additionaly relate the transversal and vectorial components via

$$\Pi^{\mu\nu}(s) = \underbrace{(q^\mu q^\nu - g^{\mu\nu}q^2)\Pi^{(T)}(s) + (q^\mu q^\nu - g^{\mu\nu}q^2)\Pi^{(L)}(s)}_{=(q^\mu q^\nu - g^{\mu\nu}q^2)\Pi^{(T+L)}(s)} + \frac{g^{\mu\nu}s^2}{q^2}\Pi^{(L)}(s), \tag{3.11}$$

such that

$$\Pi^{(V,A)}(s) = \Pi^{(T)}(s) + \Pi^{(L)} = \Pi^{(T+L)}, \tag{3.12}$$

where the vector/ axial-vector component of the correlator is now related to the newly defined transversal and longitudinal combination of the correlator. As the τ-decays, with the limiting factor of the τ-mass, can only decay into light quarks we will often neglect the quark masses and work in the so called chiral limit. In the chiral limit the longitudinal component, which is proportional to the quark masses, of the correlator vanishes.

Examining the inclusive ratio R_τ in eq. (3.1), we note that we have to deal with a problematic integral over the real axis of $\Pi(s)$ from 0 up to m_τ. The integral is problematic for two reasons:

- **Perturbative Quantum Chromodynamcs** (pQCD) and the OPE breaks down for low energies (over which we have to integrate).
- The positive euclidean axis of $\Pi(s)$ has a discontinuity cut and can theoretically not be evaluated (see section 2.1.2).

To literally circunvent the former issue we make use of *Cauchy's Theorem* eq. (2.34). For the latter we will apply so-called **pinched weights**.

3.1 Rescuing pQCD with Cauchy's theorem

We will make use of Cauchy's theorem to rewrite the definite integral of eq. (3.2) into a contour integral over a closed circle with radius m_τ^2. The closed contour consists of four line integrals, which have been visualized in fig. 3.2. Summing over the four line integrals, performing a *analytic continuation* of the two-point correlator $\Pi(s) \to \Pi(s + i\epsilon)$ and finally taking the limit of $\epsilon \to 0$ gives us the needed relation between eq. (3.2) and the closed contour:

$$\begin{aligned}
\oint_{s=m_\tau} \Pi(s) &= \int_0^{m_\tau} \Pi(s+i\epsilon) + \int_{\mathcal{C}_2} \Pi(s)\,\mathrm{d}s + \int_{m_\tau}^0 \Pi(s-i\epsilon)\,\mathrm{d}s + \int_{\mathcal{C}_4} \Pi(s)\,\mathrm{d}s \\
&= \int_0^{m_\tau} \Pi(s+i\epsilon) - \Pi(s-i\epsilon)\,\mathrm{d}s + \int_{\mathcal{C}_2} \Pi(s)\,\mathrm{d}s + \int_{\mathcal{C}_4} \Pi(s)\,\mathrm{d}s \\
&= \int_0^{m_\tau} \Pi(s+i\epsilon) - \overline{\Pi(s+i\epsilon)} + \int_{\mathcal{C}_2} \Pi(s)\,\mathrm{d}s + \int_{\mathcal{C}_4} \Pi(s)\,\mathrm{d}s \\
&\overset{\lim \epsilon \to 0}{=} 2i \int_0^{m_\tau} \operatorname{Im} \Pi(s)\,\mathrm{d}s + \oint_{s=m_\tau} \Pi(s)\,\mathrm{d}s
\end{aligned} \tag{3.13}$$

where we made use of $\Pi(z) = \overline{\Pi(\overline{z})}$ (due to $\Pi(s)$ is analytic) and $\Pi(z) - \overline{\Pi(z)} = 2i \operatorname{Im} \Pi(z)$. The result can be rewritten in a more intuitive form, which we also visualized in fig. 3.2

$$\int_0^{m_\tau} \Pi(s)\,\mathrm{d}s = \frac{i}{2} \oint_{s=m_\tau} \Pi(s)\,\mathrm{d}s \tag{3.14}$$

Due to the circle-contour we can avoid low energies at which pQCD would

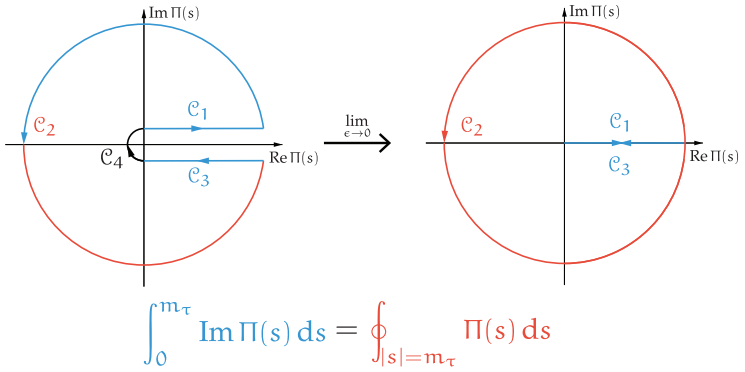

Figure 3.2: Visualization of the usage of Cauchy's theorem to transform eq. (3.2) into a closed contour integral over a circle of radius m_τ^2.

break down.

To deal with the latter issue we have to suppress the contributions of the correlator close to the positive real axis, which can be achieved by introducing weight functions, which suppress contributions of the two-point function close to the postive real axis.

Finally combining eq. (3.14) with eq. (3.2) we get

$$R_\tau = 6\pi i \oint_{s=m_\tau} \frac{\mathrm{d}s}{m_\tau^2}\left(1-\frac{s}{m_\tau^2}\right)\left[\left(1+2\frac{s}{m_\tau^2}\right)\Pi^{(T)}(s)+\Pi^{(L)}\right] \tag{3.15}$$

for the hadronic τ-decay ratio. It is convenient to work with $\Pi^{(T+L)}$, which is connected to the vector/ axial-vector components of the correlator. Thus using eq. (3.10) in eq. (3.15) yields

$$R_\tau = 6\pi i \oint_{|s|=m_\tau} \frac{\mathrm{d}s}{m_\tau^2}\left(1-\frac{s}{m_\tau^2}\right)^2\left[\left(1+2\frac{s}{m_\tau^2}\right)\Pi^{(L+T)}(s)-\left(\frac{2s}{m_\tau^2}\right)\Pi^{(L)}(s)\right] \tag{3.16}$$

By introducing Cauchy's theorem we avoided low energies, which could lead to a breakdown of PT. The contour integral obtained is an important result as we are now able to theoretically evaluate the hadronic τ-decay ratio at sufficiently large energy scales ($m_\tau \approx 1.78\,\mathrm{MeV}$) at which $\alpha_s(m_\tau) \approx 0.33$ [28] is large enough to apply perturbation theory and the OPE. Obviously we would benefit from a contour integral over a bigger circunference, but τ-decays are limited by the m_τ. Nevertheless there are promising e^+e^- annihilation data, which yields valuable R-ratio values up to 2 GeV [4][22].

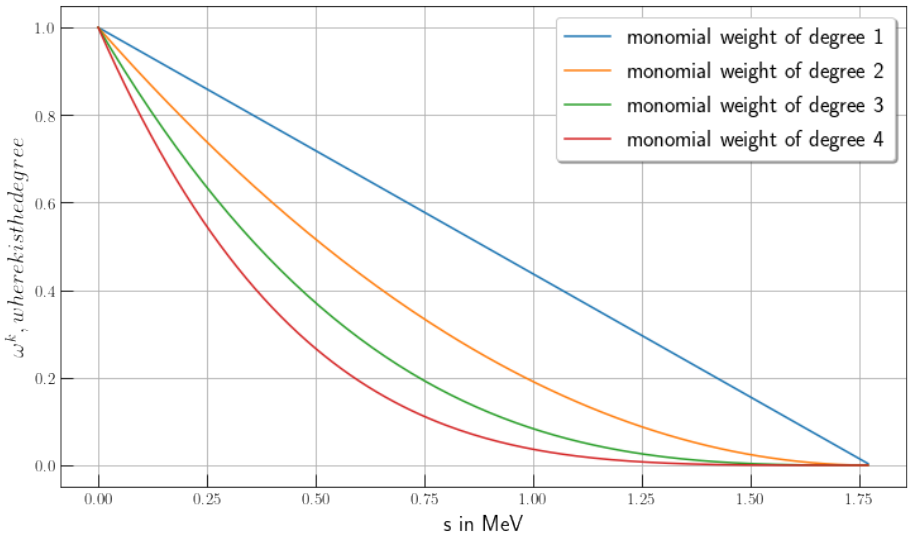

Figure 3.3: Monomial weights $(1 - s/m_\tau^2)^k$ for degrees $1 \to 4$. We can see that weights of heigher pinching decrease faster, which comes in handy if we want to suppress duality violations.

3.2 Pinched weights to avoid DVs

We are free to multiply eq. (3.14) by an analytic weight function $\omega(s)$

$$\int_0^{m_\tau} \omega(s)\Pi(s)\,\mathrm{d}s = \frac{i}{2}\oint_{s=m_\tau} \omega(s)\Pi(s)\,\mathrm{d}s. \tag{3.17}$$

We can use this technique to suppress contributions for the two-point function close to the positive real axis by implementing so called **pinched weights** of the form

$$\omega(s) = (1 - \frac{s}{m_\tau^2})^k, \tag{3.18}$$

where k is the degree of the pinched weight. The heigher the degree the farther we operate from the critical postivie real axis (see. **??**), which suppresses the effects of duality violations. This pinching of second degree appears quite naturally. If we regard the incluse $\tau - decay$ ratio eq. (3.15), we note that for the transversal component we already have a double pinched weight, the *kinematic weight*

$$\omega_\tau(s) = \left(1 - \frac{s}{m_\tau^2}\right)\left(1 + 2\frac{s}{m_\tau^2}\right). \tag{3.19}$$

In general it is said that a double pinched weight is sufficient to neglect effects caused by duality violation.

We can also use different weights to control the dimensions of the OPE that contribute. The weights we are using have to be analytic, so that we can make

monomial:	x^0	x^1	x^2	x^3	x^5	x^6	x^7
dimension:	$D^{(2)}$	$D^{(4)}$	$D^{(6)}$	$D^{(8)}$	$D^{(10)}$	$D^{(12)}$	$D^{(14)}$

Table 3.2: List of monomials and their corresponding "active" dimensions in the OPE.

use of Cauchy's theorem. Thus they can be represented as polynomials

$$\omega(x) = \sum_i a_i x^i, \tag{3.20}$$

every contributing monomial is responsible for a dimension of the OPE. Dimensions that are not represented in the weight polynomial do not contribute at all or are very suppressed as we will demonstrate now.

The residue of a monomial x^k is only different from 0 if its power $k = -1$:

$$\oint_C x^k \,\mathrm{d}x = i \int_0^{2\pi} \left(e^{i\theta}\right)^{k+1} \mathrm{d}\theta = \begin{cases} 2\pi i & \text{if } k = -1, \\ 0 & \text{otherwise} \end{cases}. \tag{3.21}$$

Consequently if we exchange the kinematic weight of the incluse ratio eq. (3.1) through a monomial and neglect all terms of no interest to us we can write

$$\begin{aligned} R(xm_\tau)\big|_{D=0,2,4\ldots} &= \oint_{|x|=1} \frac{x^k}{(xm_\tau)^{\frac{D}{2}}} C^D(xm_\tau) \\ &= \frac{1}{(m_\tau)^{\frac{D}{2}}} \oint_{|x|=1} x^{k-D/2}\, C^D(xm_\tau), \end{aligned} \tag{3.22}$$

where C^D are the D-dimensional Wilson coefficients. Thus combining eq. (3.21) with eq. (3.22) we see that only Dimension which fulfill

$$k - D/2 = -1 \quad \Longrightarrow \quad D = 2(k+1) \tag{3.23}$$

contribute to the OPE. For example the polynomial of the kinematic weight is given by

$$(1-x)^2(1+2x) = \underbrace{1}_{D=2} - 3\underbrace{x^2}_{D=6} + 2\underbrace{x^3}_{D=8}, \tag{3.24}$$

where we underbraced the monomials and gave the active dimensions. A list of monomomials and their corresponding Dimensions up to dimension 14 can be found in table 3.2. This behaviour enables us to bring out different dimensions of the OPE and suppress contributions of heigher order ($D \geq 10$) for which less is kown.

3.3 RG invariance

The two-point function is not a physical quantity. It does not fulfill the RGE eq. (2.4) and is thus dependent on the scale μ. We can enhance the inclusive

ration eq. (3.1) making use of the **Adler function** defined as:

$$D^{(T+L)}(s) \equiv -s\frac{\mathrm{d}}{\mathrm{d}s}\Pi^{(T+L)}(s), \qquad D^{(L)}(s) \equiv \frac{s}{m_\tau^2}\frac{\mathrm{d}}{\mathrm{d}s}(s\Pi^{(L)}(s)), \tag{3.25}$$

where we have two separate definitions: one for the transversal plus longitudinal contribution and one for solely longitudinal part. The two-point functions can now be replaced with the help of partial integration

$$\int_a^b u(x)V(x)\,\mathrm{d}x = \big[U(x)V(x)\big]_a^b - \int_a^b U(x)v(x)\,\mathrm{d}x. \tag{3.26}$$

We will do the computation for each of the two cases $(T+L)$ and (L) separate. Starting by the transversal plus longitudinal contribution we get:

$$\begin{aligned} R_\tau^{(1)} &= \frac{6\pi i}{m_\tau^2}\oint_{|s|=m_\tau^2} \underbrace{\left(1-\frac{s}{m_\tau^2}\right)^2\left(1+2\frac{s}{m_\tau^2}\right)}_{=u(x)}\underbrace{\Pi^{(L+T)}(s)}_{=V(x)} \\ &= \frac{6\pi i}{m_\tau^2}\left\{\left[-\frac{m_\tau^2}{2}\left(1-\frac{s}{m_\tau^2}\right)^3\left(1+\frac{s}{m_\tau^2}\right)\Pi^{(L+T)}(s)\right]_{|s|=m_\tau^2}\right. \\ &\quad \left. + \oint_{|s|=m_\tau^2}\underbrace{-\frac{m_\tau^2}{2}\left(1-\frac{s}{m_\tau^2}\right)^3\left(1+\frac{s}{m_\tau^2}\right)}_{=U(x)}\underbrace{\tfrac{\mathrm{d}}{\mathrm{d}s}\Pi^{(L+T)}(s)}_{=v(x)}\right\} \\ &= -3\pi i\oint_{|s|=m_\tau^2 s}\frac{\mathrm{d}s}{s}\left(1-\frac{s}{m_\tau^2}\right)^3\left(1+\frac{s}{m_\tau^2}\right)\tfrac{\mathrm{d}}{\mathrm{d}s}D^{(L+T)} \end{aligned} \tag{3.27}$$

where we fixed the integration constant to $C = -\frac{m_\tau^2}{2}$ in the second line and left the antiderivatives contained in the squared brackets untouched. If we parametrizing the integral appearing in the expression in the squared brackets we can derive that it vanishes:

$$\left[-\frac{m_\tau^2}{2}\left(1-e^{-i\phi}\right)^3\left(1+e^{-i\phi}\right)\Pi^{(L+T)}(m_\tau^2 e^{-i\phi})\right]_0^{2\pi} = 0 \tag{3.28}$$

where $s \to m_\tau^2 e^{-i\phi}$ and $(1-e^{-i\cdot 0}) = (1-e^{-i\cdot 2\pi}) = 0$. Repeating the same calculation for the longitudinal part yields

$$\begin{aligned} R_\tau^{(L)} &= \oint_{|s|=m_\tau^2}\mathrm{d}s\left(1-\frac{s}{m_\tau^2}\right)^2\left(-\frac{2s}{m_\tau^2}\right)\Pi^{(L)}(s) \\ &= -4\pi i\oint\frac{\mathrm{d}s}{s}\left(1-\frac{s}{m_\tau^2}\right)^3 D^{(L)}(s) \end{aligned} \tag{3.29}$$

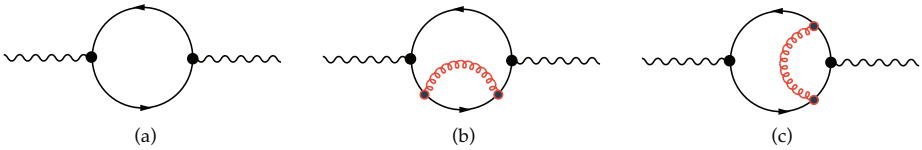

Consequently combining the two parts results in

$$R_\tau = -\pi i \oint_{|s|=m_\tau^2} \frac{\mathrm{d}s}{s} \left(1 - \frac{s}{m_\tau^2}\right)^3 \left[3\left(1 + \frac{s}{m_\tau^2} D^{(L+T)}(s) + 4D^{(L)}(s)\right)\right]. \tag{3.30}$$

It is convenient to define $x = s/m_\tau^2$ such that we can rewrite the inclusive ratio as

$$R_\tau = -\pi i \oint_{|s|=m_\tau^2} \frac{\mathrm{d}x}{x} (1-x)^3 \left[3(1+x) D^{(L+T)}(m_\tau^2 x) + 4D^{(L)}(m_\tau^2 x)\right]. \tag{3.31}$$

$$R^\omega_{\tau,V/A} = \frac{N_c}{2} S_{EW} |V_{ud}|^2 \left(1 + \delta^{(0)}_\omega + \delta^{EW}_\omega + \delta^{DVs}_\omega + \sum_{D\leq 2} \delta^{(D)}_{ud,\omega}\right) \tag{3.32}$$

3.4 The perturbative expansion

We will treat the correlator in the chiral limit for which the longitudinal components $\Pi^L(s)$ vanish (see eq. (3.11)) and the axial and vectorial contributions are equal. In the massless case we then can write the vector correlation function $\Pi(s)$ as [2]:

$$\Pi_V^{T+L}(s) = -\frac{N_c}{12\pi^2} \sum_{n=0}^{\infty} a_\mu^n \sum_{k=0}^{n+1} c_{n,k} L^k \quad \text{with} \quad L \equiv \ln \frac{-s}{\mu^2}. \tag{3.33}$$

The coeffiecient $c_{n,k}$ up to two-loop order can be obtained by Feynman-diagram calculations. add complete calculation E.g. we can compare the zero-loop result of the correlator [19]

$$\Pi^B_{\mu\nu}(q^2)\Big|^{1-loop} = \frac{N_c}{12\pi^2} \left(\frac{1}{\hat{\epsilon}} - \log \frac{(-q^2 - i0)}{\mu^2} + \frac{5}{3} + \mathcal{O}(\epsilon)\right) \tag{3.34}$$

with eq. (3.33) and extract the first two coefficients

$$c_{00} = -\frac{5}{3} \qquad \text{and} \qquad c_{01} = 1, \tag{3.35}$$

where $\Pi^B_{\mu\nu}(q^2)$ is not renormalized[3]

[3]The term $1/\hat{\epsilon}$, which is of order 0 in α_s, will be cancelled by renormalization.

The second loop can also be calculated by diagram techniques resulting in [3]

$$\Pi_V^{(1+0)}(s)\Big|^{2-loop} = -\frac{N_c}{12\pi^2} a_\mu \log(\frac{-s}{\mu^2}) + \cdots \tag{3.36}$$

yielding $c_{11} = 1$.

Beginning from three loop diagrams the algebra becomes exausting and one has to use dedicated algorithms to compute the heigher loops. The third loop calculations have been done in the late seventies by [11, 16, 10]. The four loop evaluation have been completed a little more than ten years later by [17, 34]. The heighest loop published, that amounts to α_s^4, was published in 2008 [1] almost 20 years later.

Fixing the number of colors to $N_c = 3$ the missing coefficients up to order four in α_s read:

$$\begin{aligned}
c_{2,1} &= \frac{365}{24} - 11\zeta_3 - \left(\frac{11}{12} - \frac{2}{3}\zeta_3\right) N_f \\
c_{3,1} &= \frac{87029}{288} - \frac{1103}{4}\zeta_3 + \frac{275}{6}\zeta_5 \\
&\quad - \left(\frac{7847}{216} - \frac{262}{9}\zeta_3 + \frac{25}{9}\zeta_5\right) N_f + \left(\frac{151}{162} - \frac{19}{27}\zeta_3\right) N_f^2 \\
c_{4,1} &= \frac{78631453}{20736} - \frac{1704247}{432}\zeta_3 + \frac{4185}{8}\zeta_3^2 + \frac{34165}{96}\zeta_5 - \frac{1995}{16}\zeta_7,
\end{aligned} \tag{3.37}$$

where used the flavour number $N_f = 3$ for the last line.

The 6-loop calculation has until today not been achieved, but Beneke und Jamin [2] used and educated guess to estimate the coefficient

$$c_{5,1} \approx 283 \pm 283. \tag{3.38}$$

Until now we have given the coefficients $c_{n,k}$ with solely $k = 1$. This is due to the RGE, which relates coefficients with k different than one to the coefficients mentioned above. To make use of the RGE the correlator $\Pi_V^{T+L}(s)$ needs to be a physical quantity, which can be achieved by rewriting it in terms of the Adler function (see. eq. (3.25)) to:

$$D_V^{(T+L)} = -s\frac{\mathrm{d}\Pi_V^{(T+L)}(s)}{\mathrm{d}s} = \frac{N_c}{12\pi^2}\sum_{n=0}^{\infty} a_\mu^n \sum_{k=1}^{n+1} k c_{n,k} L^{k-1}, \tag{3.39}$$

where we used $\mathrm{d}L^k/\,\mathrm{d}s = k\ln(-s/\mu^2)^{k-1}(-1/\mu^2)$. The Adler-function is physical quantity and has to fulfill the RGE eq. (2.4):

$$-\mu\frac{\mathrm{d}}{\mathrm{d}\mu}D_V^{(T+L)} = -\mu\frac{\mathrm{d}}{\mathrm{d}\mu}\left(\tfrac{\partial}{\partial L}\,\mathrm{d}L + \tfrac{\partial}{\partial a_s}\,\mathrm{d}a_s\right) D_V^{T+L} = \left(2\tfrac{\partial}{\partial L} + \beta\tfrac{\partial}{\partial a_s}\right) D_V^{T+L} = 0, \tag{3.40}$$

where we defined the β-function in eq. (2.5) and used $\mathrm{d}L/\,\mathrm{d}\mu = -2/\mu$. The RGE puts constraints on the $c_{n,k}$-coefficients for different ks, which are not not independent anymore.

For example writing out the sum of the adler function to the second order in α_s yields

$$D(s) = \frac{N_c}{12\pi^2}\left[c_{01} + a_\mu(c_{11} + 2c_{12}L) + a_\mu^2(c_{21} + 2c_{22}L + 3c_{23}L^2)\right]. \tag{3.41}$$

Then inserting eq. (3.41) into the RGE

$$4a_\mu c_{12} + 2a_\mu^2(2c_{22} + 6c_{23}L) + \beta_1 a_\mu^2(c_{11} + 2c_{12}L) + \mathcal{O}(a_\mu^3) = 0 \tag{3.42}$$

lets us compare the coefficients order by order in α_s. At order α_μ only the c_{12} term is present and has to be zero consequently. For $\mathcal{O}(a_\mu^2 L)$ the only c_{23} exists ($c_{12} = 0$) and has to vanish as well. Finally at $\mathcal{O}(a)$ we can relate c_{22} with c_{11} resulting in:

$$c_{12} = 0, \quad c_{22} = \frac{\beta_1 c_{11}}{4} \quad \text{and} \quad c_{23} = 0. \tag{3.43}$$

or $D(s)$ to the first order in α_s. Implementing the newly obtained Adler-coefficients we can write out the adler function to the first order:

$$D(s) = \frac{N_c}{12\pi^2}\left[c_{01} + c_{11}a_\mu\left(c_{21} - \frac{1}{2}\beta_1 c_{11}L\right)a_\mu^2\right] + \mathcal{O}(a_\mu^3). \tag{3.44}$$

We have used the RGE to relate Adler-function coefficients and thus reduce its numbers. But as we will see in the following section the RGE gives us two different choices in the order of the computation of the perturbative contribution to the inclusive τ-decay ratio.

3.4.1 Renormalisation group summation

By making use of the RGE we have to decide about the order of mathematical operations we perform. As the perturbative contribution $\delta^{(0)}$ is independent on the scale μ we are confronted with two choices **fixed-order perturbation theory** (FOPT) or **contour-improved perturbation theory**. Each of them yields a different result and is the main source of error in extracting the strong coupling from τ-decays.

We can write the perturbative contribution $\delta^{(0)}$ to R_τ (see eq. (3.32)) in the chiral limit, such that $D^{(L)}$ vanishes as

$$\delta^{(0)} = \sum_{n=1}^{\infty} a_\mu^n \sum_{k=1}^{n} k c_{n,k} \frac{1}{2\pi i}\oint_{|x|=1} \frac{\mathrm{d}x}{x}(1-x)^3(1+x)\log\left(\frac{-M_\tau^2 x}{\mu^2}\right)^{k-1}, \tag{3.45}$$

where we inserted the expansion of $D_V^{(T+L)}$ eq. (3.25) into R_τ eq. (3.31). Keep in mind that the contributions from the vector and axialvector correlator are identical in the massless case:

$$D^{(T+L)} = D_V^{(T+L)} + D_A^{(T+L)} = 2D_V^{(T+L)}. \tag{3.46}$$

In the following we will explain both the descriptions, starting by FOPT. By using the FOPT prescription we fix $\mu^2 = m_\tau^2$ leading to

$$\delta_{FO}^{(0)} = \sum_{n=1}^{\infty} a(m_\tau^2)^n \sum_{k=1}^{n} k c_{n,k} J_{k-1} \tag{3.47}$$

where the contour integrals J_l are defined by

$$J_l \equiv \frac{1}{2\pi i} \oint_{|x|=1} \frac{\mathrm{d}x}{x} (1-x)^3 (1+x) \log^l(-x). \tag{3.48}$$

The integrals J_l up to order α_s^4 are given by [2]:

$$J_0 = 1, \quad J_1 = -\frac{19}{12} \quad J_2 = \frac{265}{72} - \frac{1}{3}\pi^2, \quad J_3 = -\frac{3355}{288} + \frac{19}{12}\pi^2. \tag{3.49}$$

Using FOPT the strong coupling $a(\mu)$, which runs with the scale μ, is fixed at $a(m_\tau^2)$ and can be taken out of the closed-contour integral. Thus we solely to integrate over the logarithms $\log(-s/m_\tau^2)$.

Using CIPT we can sum the logarithms by setting the scale to $\mu^2 = -m_\tau^2 x$ in eq. (3.45), resulting in:

$$\delta_{CI}^{(0)} = \sum_{n=1}^{\infty} c_{n,1} J_n^a(m_\tau^2), \tag{3.50}$$

where the contour integrals J_l are defined by

$$J_n^a(m_\tau^2) \equiv \frac{1}{2\pi i} \oint_{|x|=1} \frac{\mathrm{d}x}{x} (1-x)^3 (1+x) a^n(-m_\tau^2 x). \tag{3.51}$$

All logarithms vanish except the ones for $k = 1$:

$$\log(1)^{k-1} = \begin{cases} 1 & \text{if } k = 1, \\ 0 & k \neq 1 \end{cases} \tag{3.52}$$

which selectes adler function coefficients $c_{n,1}$ with a fixed $k = 1$. Handling the logarithms left us with the integration of $\alpha_s(-m_\tau^2 x)$ over the closed-contour $\oint_{|x|=1}$, which now depends on the integration variable x. In general we have to decide if we want to perform a contour integration with a constant coupling constant and variable logarithms (FOPT) or "constant logarithms" and a running coupling (CIPT).

To emphasize the differences in both approaches we can calculate the perturbative contribution $\delta^{(0)}$ to R_τ for the two different prescriptions yielding [2]

$$\begin{aligned} & \alpha_s^2 \quad \alpha_s^2 \quad \alpha_s^3 \quad \alpha_s^4 \quad \alpha_s^5 \\ \delta_{FO}^{(0)} &= 0.1082 + 0.0609 + 0.0334 + 0.0174(+0.0088) = 0.2200(0.2288) \quad (3.53) \\ \delta_{CI}^{(0)} &= 0.1479 + 0.0297 + 0.0122 + 0.0086(+0.0038) = 0.1984(0.2021). \quad (3.54) \end{aligned}$$

The series indicate, that CIPT converges faster and that both series aproach a different value. This discrepancy represents currently the biggest theoretical uncertainity while extracting the strong coupling α_s.

As today we do not know if FOPT or CIPT is the correct approach of measuring α_s. Therefore there are currently three ways of stating results:

- Quoting the average of both results.
- Quoting the CIPT result.
- Quoting the FOPT result.

We follow the approach of Beneke and Jamin [**Benke2008**] who have shown advantages of FOPT over CIPT.

3.5 Non-Perturbative OPE Contribution

The perturbative contribution to the Sum-Rule, that we have seen so far, is the dominant one. With

$$\begin{aligned} R_\tau^{FOPT} &= \\ R_\tau^{CIPT} &= \end{aligned} \tag{3.55}$$

The NP vs perturbative contributions can be varied by choosen different weights than ω_τ.

3.5.1 Dimension four

For the OPE contributions of dimension four we have to take into account the terms with masses to the fourth power m^4, the quark condensate multiplied by a mass $m\langle\overline{q}\,q\rangle$ and the glucon condensate $\langle GG\rangle$. The resulting expression can be taken from the appendix of [**Pich1999**], yielding:

$$D_{ij}^{(L+T)}(s)\Big|_{D=4} = \frac{1}{s^2}\sum_n \Omega^{(1+0)}(s/\mu^2)a^n, \tag{3.56}$$

where

$$\begin{aligned} \Omega_n^{(1+0)}(s/\mu^2) \;=\; & \frac{1}{6}\langle aGG\rangle p_n^{(L+T)}(s/\mu^2) + \sum_k m_k\langle\overline{q}_{\,k}q_k\rangle r_n^{(L+T)}(s/\mu^2) \\ & + 2\langle m_i\overline{q}_{\,i}q_i + m_j\overline{q}_{\,j}q_j\rangle q_n^{(L+T)}(s/\mu^2) \pm \frac{8}{3}\langle m_j\overline{q}_{\,i}q_i + m_i\overline{q}_{\,j}q_j\rangle t_n^{(L+T)} \\ & - \frac{3}{\pi^2}(m_i^4 + m_j^4)h_n^{(L+T)}(s/\mu^2) \mp \frac{5}{\pi^2}m_i m_j(m_i^2 + m_j^2)k_n^{(L+T)}(s/\mu^2) \\ & + \frac{3}{\pi^2}m_i^2 m_j^2 g_n^{(L+T)}(s/\mu^2) + \sum_k m_k^4 j_n^{(L+T)}(s/\mu^2) + 2\sum_{k\neq l} m_k^2 m_l^2 u_n^{(L+T)}(s/\mu^2) \end{aligned} \tag{3.57}$$

The perturbative expansion coefficients are known to $\mathcal{O}(a^2)$ for the condensate contributions,

$$\begin{array}{lll} p_0^{(L+T)} = 0, & p_1^{(L+T)} = 1, & p_2^{(L+T)} = \frac{7}{6}, \\ r_0^{(L+T)} = 0, & r_1^{(L+T)} = 0, & r_2^{(L+T)} = -\frac{5}{3} + \frac{8}{3}\zeta_3 - \frac{2}{3}\log(s/\mu^2), \\ q_0^{(L+T)} = 1, & q_1^{(L+T)} = -1, & q_2^{(L+T)} = -\frac{131}{24} + \frac{9}{4}\log(s/\mu^2) \\ t_0^{(L+T)} = 0 & t_1^{(L+T)} = 1, & t_2^{(L+T)} = \frac{17}{2} + \frac{9}{2}\log(s/\mu^2). \end{array} \tag{3.58}$$

while the m^4 terms have been only computed to $\mathcal{O}(a)$

$$\begin{array}{ll} h_0^{(L+T)} = 1 - 1/2\log(s/\mu^2), & h_1^{(L+T)} = \frac{25}{4} - 2\zeta_3 - \frac{25}{6}\log(s/\mu^2) - 2\log(s/\mu^2)^2, \\ k_0^{(L+T)} = 0, & k_1^{(L+T)} = 1 - \frac{2}{5}\log(s/\mu^2), \\ g_0^{(L+T)} = 1, & g_1^{(L+T)} = \frac{94}{9} - \frac{4}{3}\zeta_3 - 4\log(s/\mu^2), \\ j_0^{(L+T)} = 0, & j_1^{(L+T)} = 0, \\ u_0^{(L+T)} = 0, & u_2^{(L+T)} = 0. \end{array} \tag{3.59}$$

3.5.2 Dimension six and eight

Our application of dimension six contributions is founded in [6] and has previously been calculated beyond leading order by [23]. The operators appearing are the masses to the power six m^6, the four-quark condensates $\langle \overline{q}\, q \overline{q}\, q \rangle$, the three-gluon condensates $\langle g^3 G^3 \rangle$ and lower dimensional condensates multiplies by the corresponding masses, such that in total the mass dimension of the operator will be six. As there are too many parameters to be fitted with experimental data we have to omit some of them, starting with the three-gluon condensate, which does not contribute at leading order. The four-quark condensates known up to $\mathcal{O}(a^2)$, but we will make use of the *vacuum saturation approach* [2, 6, 33] to express them in quark, anti-quark condensates $\langle q\overline{q} \rangle$. In our work we take the simplest approach possible: Introducing an effective dimension six coefficient $\rho_{V/A}^{(6)}$ divided by the appropiate power in s

$$D_{ij,V/A}^{(1+0)}\Big|_{D=6} = 0.03 \frac{\rho_{V/A}^{(6)}}{s^3} \tag{3.60}$$

As for the dimension eigth contribution the situation is not better than the dimension six one we keep the simplest approach, leading to

$$D_{ij,V/A}^{(1+0)}\Big|_{D=8} = 0.04 \frac{\rho_{V/A}^{(8)}}{s^4}. \tag{3.61}$$

3.5.3 Duality Violations

3.6 Experiment

The τ-decay data we use to perform our QCD-analysis is from the **ALEPH** experiment. The ALEPH experiment was located at the large-electron-positron

(LEP) collider at CERN laboratory in Geneva. LEP started producing particles in 1989 and was replaced in the late 90s by the large-hadron-collider, which makes use of the same tunnel of 27km circumference. The data produced within the experiment is still maintained by former ALEPH group members under led by M. Davier, which have performed regular updates on the data-sets [15, 12, 30].

The measured spectral functions for the Aleph data are defined in [13] and given for the transversal and longitudinal components separatly:

$$\begin{aligned}\rho_{V/A}^{(T)}(s) &= \frac{m_\tau^2}{12\left|V_{ud}^2\right| S_{EW}} \frac{\mathcal{B}(\tau^- \to V^-/A^- \nu_\tau)}{\mathcal{B}(\tau^- \to e^- \overline{\nu}_e \nu_\tau)} \\ &\quad \times \frac{\mathrm{d}N_{V/A}}{N_{V/A}\,\mathrm{d}s} \left[\left(1 - \frac{s}{m_\tau^2}\right)^2 \left(1 + \frac{2s}{m_\tau^2}\right)\right]^{-1} \qquad (3.62) \\ \rho_A^{(L)}(s) &= \frac{m_\tau^2}{12\left|V_{ud}^2 S_{EW}\right|} \frac{\mathcal{B}(\tau^- \to \pi^-(K^-)\nu_\tau)}{\mathcal{B}(\tau^- \to e^- \overline{\nu}_e \nu_\tau)} \times \frac{\mathrm{d}N_A}{N_A\,\mathrm{d}s} \left(1 - \frac{s}{m_\tau^2}\right)^{-2}.\end{aligned}$$

$$\mathcal{B}_e = ... \qquad (3.63)$$

$$R_{\tau,V/A} = \frac{B_{V/A,\tau}}{B_e} \qquad (3.64)$$

The data relies on a separation into vector and axial-vector channels. In the case of the Pions this can be achieved via counting. The vector channel is characterized by a negative parity, whereas the axial-vector channel has positive parity. A quark has by definition positive parity, thus an anti-quark has a negative parity. A meson, like the Pion particle, is a composite particle consiting of an quark an anti-quark. Consequently a single Pion carries negative parity, an even number of Pions carries positive parity and an odd number of Pions carries negative parity:

$$n \times \pi = \begin{cases} \text{vector} & \text{if } n \text{ is even,} \\ \text{axial-vector} & \text{otherwise} \end{cases}. \qquad (3.65)$$

The contributions to the vector and axial channel can be seen in figure. The dominant modes in the vector case are [14] $\tau^- \to \pi^-\pi^0\nu_\tau$ and the $\tau^- \to \pi^-\pi^-\pi^+\pi^0\nu_\tau$. The first of these is produced by the $\rho(770)$ meson, which in contrary to the pions carries angular momentum of one, which is also clearly visible as peak around 770 GeV in figure vector. The dominant modes in the axial-vector case are $\tau^- \to \pi^-\nu_\tau$, $\tau^- \to \pi^-\pi^0\pi^0\nu_\tau$ and $\tau^- \to \pi^-\pi^-\pi^+\nu_\tau$. Here the three pion final states stem from the a_1^--meson, which is also clearly visible as a peak in figure.

wavy =¿ DV OPE cannot reproduce suppressed in VpA regions below 1.5 GeV can still not be applied

The different inclusive τ-decay ratios are then given by

$$R_{\tau,V} = ... \qquad (3.66)$$

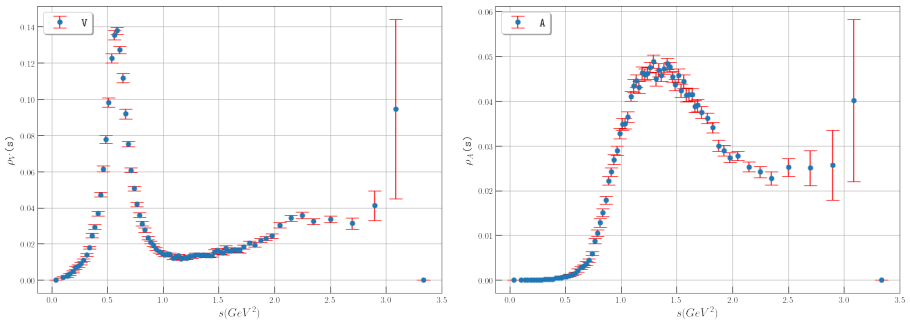

(a) A gull (b) A mouse

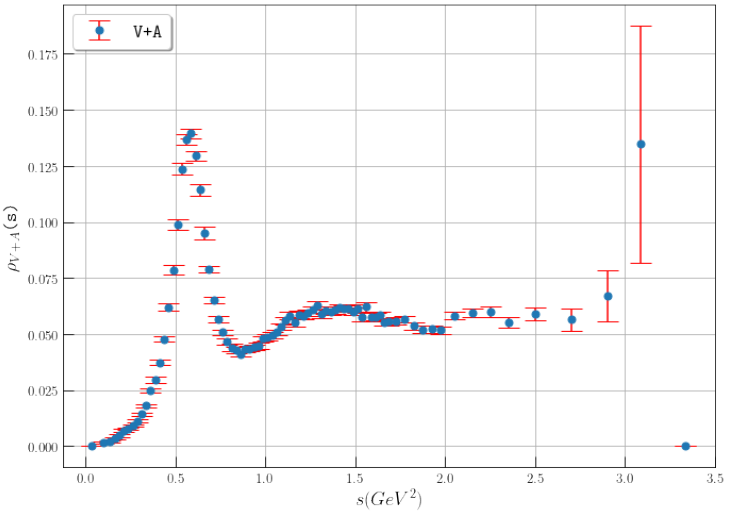

Figure 3.4: Pictures of animals

3.7 Fits

3.7.1 Kinematic weight: $\omega(x) = (1-x)^2(1+2x)$

The kinematic weight $\omega(x) = (1-x)^2(1+2x)$ is the natural appearing weight carried by the eq. (3.1). Its polinomial contains terms proportional to x^2 and x^3 which makes it sensitive to $D = 6$ and $D = 8$ contributions from the OPE. Consequently we fitted the strong coupling $\alpha_s(m_\tau^2)$ and the OPE coefficients for dimension six and eight. The fits have been performed within the framework of FOPT for different numbers of s_0. The momentum sets are characterized by its lowest energy s_{min}. We fitted values up to 1.5 GeV, as including more moments causes problems with the convergence of our fitting routine. This is due to their heigh correlation which has been plotted in correlation plot?? Going to lower energies also bares the risk to be affected by the $\rho(770)$ and a_1 peaks in the vector and axial-vector spectral function. We have given all of our fit values in table 3.3 and fig. 3.5.

s_{min}	$\#s_0$s	$\alpha_s(m_\tau^2)$	c_6	c_8	χ^2/dof
1.500	23	0.3255(13)	-0.441(10)	-0.2909(34)	2.00
1.525	22	0.3255(18)	-0.440(36)	-0.288(45)	2.10
1.550	21	0.3265(16)	-0.478(36)	-0.343(50)	1.81
1.575	20	0.3269(22)	-0.493(47)	-0.365(58)	1.86
1.600	19	0.3272(23)	-0.506(51)	-0.384(64)	1.94
1.625	18	0.3284(24)	-0.540(53)	-0.433(68)	1.788
1.650	17	0.3283(24)	-0.550(57)	-0.448(74)	1.90
1.675	16	0.3284(24)	-0.549(57)	-0.448(79)	2.04
1.700	15	0.3281(24)	-0.538(63)	-0.430(87)	2.19
1.750	14	0.3291(26)	-0.581(71)	-0.50(10)	2.21
1.800	13	0.3293(27)	-0.589(77)	-0.51(11)	2.43
1.850	12	0.3281(28)	-0.537(85)	-0.42(13)	2.5
1.900	11	0.3272(29)	-0.493(93)	-0.35(15)	2.65
1.950	10	0.3232(32)	-0.31(11)	-0.01(18)	1.13
2.000	9	0.3234(34)	-0.32(12)	-0.03(21)	1.31
2.100	8	0.3256(38)	-0.43(15)	-0.25(28)	1.30
2.200	7	0.3308(44)	-0.72(20)	-0.85(38)	0.19
2.300	6	0.3304(52)	-0.69(25)	-0.80(50)	0.25
2.400	5	0.3339(70)	-0.91(39)	-1.29(83)	0.10
2.600	4	0.3398(15)	-1.3(1.0)	-2.3(2.5)	0.01

Table 3.3: Table of our fitting values of $\alpha_s(m_\tau^2), c_6$ and c_8 for the kinematic weight $\omega(x) = (1-x)^2(1+2x)$ using FOPT ordered by increasing s_{min}. The errors are given in parenthesis after the observed value.

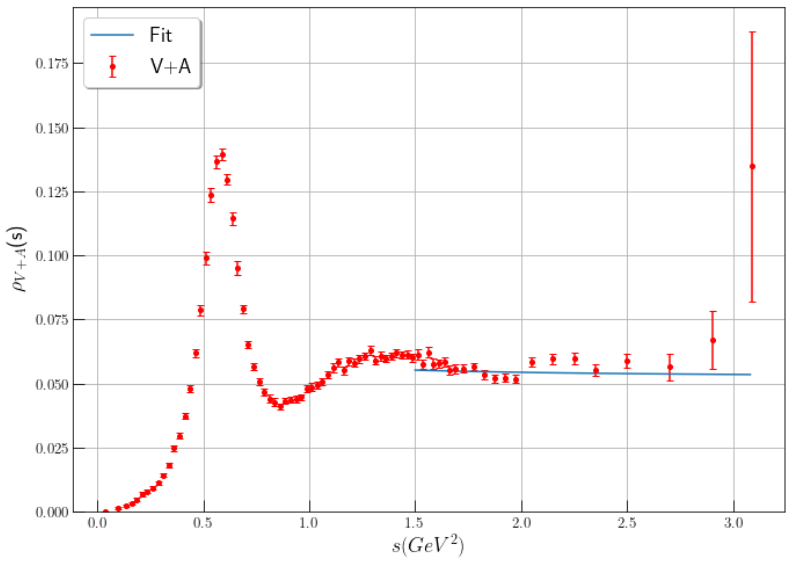

Figure 3.6: test

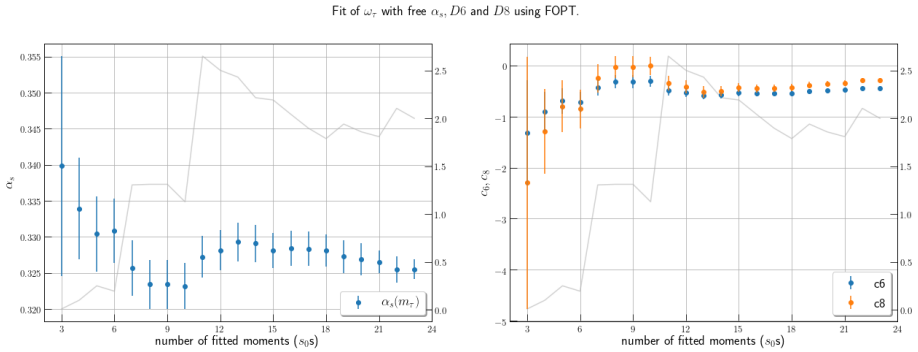

Figure 3.5: Fitting values of $\alpha_s(m_\tau^2), c_6$ and c_8 for the kinematic weight $\omega(x) = (1-x)^2(1+2x)$ using FOPT for different s_{min}. The left graph plots $\alpha_s(m_\tau^2)$ for different numbers of used s_0s. The right plot contains the dimension six and eight contributions to the OPE. Both plots have in gray the χ^2 per degree of freedom (dof).

The fits are very stable as we can see in table 3.3 and **??**. The obtained values for $\alpha_s(m_\tau^2)$ are very consitent and vary little. Their standard derivation is of order 10^{-4}. Furthermore the errors of the strong coupling are small. The

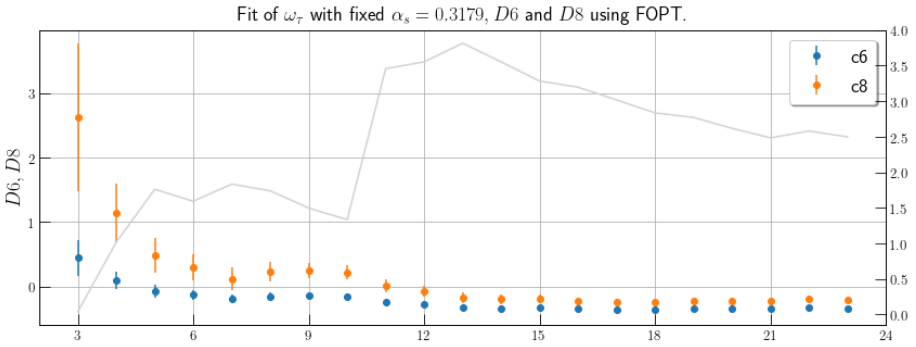

averaged relative error is as small as 1% for all of the fits. The χ^2 per **degree of freedom** (dof) is good and has its best value of 1.13 for $8 - s_0$s moments for $s_{min} = 1.95$. All of the values have a converging OPE, meaning that the values of c_8 are of the order 10 smaller than values of c_6.

D6, D8 stability

3.7.2 Cubic weight: $\omega(x) = (1-x)^3(1+3x)$

s_{min}	$\#s_0$s	$\alpha_s(m_\tau^2)$	c_6	c_8	c_{10}	χ^2/dof
1.800	13	0.3305(37)	-0.493(76)	-0.48(12)	-0.66(20)	2.99
1.850	12	0.3303(37)	-0.482(68)	-0.456(100)	-0.62(17)	3.35
1.900	11	0.3249(29)	-0.280(20)	-0.088(21)	0.088(55)	1.58
1.950	10	0.3237(26)	-0.232(25)	0.005(42)	0.275(93)	1.67
2.000	9	0.3228(26)	-0.196(27)	0.075(28)	0.420(56)	1.96
2.100	8	0.3302(40)	-0.52(11)	-0.58(22)	-1.00(45)	0.43
2.200	7	0.3312(43)	-0.56(12)	-0.68(23)	-1.23(50)	0.55
2.300	6	0.336(11)	-0.78(47)	-1.17(98)	-2.38(22)	0.29
2.400	5	0.3330(96)	-0.63(47)	-0.82(10)	-1.51(26)	0.48

Table 3.4: Table of our fitting values of $\alpha_s(m_\tau^2), c_6$, c_8 and c_{10} for the cubic weight $\omega(x) = (1-x)^3(1+3x)$ using FOPT ordered by increasing s_{min}. The errors are given in parenthesis after the observed value.

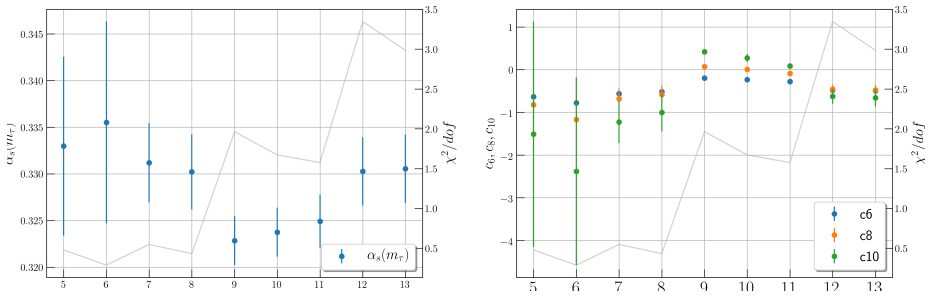

3.7.3 Quartic weight: $\omega(x) = (1-x)^4(1+4x)$

s_{min}	$\#s_0$s	$\alpha_s(m_\tau^2)$	c_6	c_8	c_{10}	χ^2/dof
1950	10	0.3308(12)	-0.3499(62)	-0.2453(55)	-0.1779(45)	1.21
2000	9	0.3290(99)	-0.3030(44)	-0.1874(30)	-0.1207(44)	0.54
2100	8	0.3278(12)	-0.2749(48)	-0.1515(28)	-0.0841(47)	0.48
2200	7	0.3286(28)	-0.296(40)	-0.181(48)	-0.117(49)	0.51
2300	6	0.3304(30)	-0.352(54)	-0.262(71)	-0.210(79)	0.41

Table 3.5: Table of our fitting values of $\alpha_s(m_\tau^2), c_6$, c_8 and c_{10} for the quartic weight $\omega(x) = (1-x)^4(1+4x)$ using FOPT ordered by increasing s_{min}. The errors are given in parenthesis after the observed value.

3.7.4 Single pinched third power monomial: $\omega(x) = 1 - x^3$

s_{min}	$\#s_0$s	$\alpha_s(m_\tau^2)$	c_8	χ^2/dof
1.500	23	0.3160(28)	-0.523(65)	2.4
1.525	22	0.3171(28)	-0.578(70)	2.3
1.550	21	0.3173(29)	-0.587(76)	2.42
1.575	20	0.3187(29)	-0.667(82)	2.08
1.600	19	0.3189(30)	-0.679(87)	2.19
1.625	18	0.3195(30)	-0.719(94)	2.24
1.650	17	0.3205(30)	-0.783(99)	2.1
1.675	16	0.3204(31)	-0.77(11)	2.24
1.700	15	0.3206(31)	-0.79(11)	2.39
1.750	14	0.3202(32)	-0.76(13)	2.57
1.800	13	0.3217(33)	-0.88(14)	2.41
1.850	12	0.3202(35)	-0.75(16)	2.4
1.900	11	0.3202(36)	-0.75(18)	2.67
1.950	10	0.3161(38)	-0.40(20)	1.46
2.000	9	0.3148(39)	-0.28(22)	1.47
2.100	8	0.3147(44)	-0.27(29)	1.71
2.200	7	0.3214(49)	-1.01(39)	0.41
2.300	6	0.3227(57)	-1.18(54)	0.46
2.400	5	0.3257(67)	-1.58(74)	0.39
2.600	4	0.325(10)	-1.54(1.53)	0.58
2.800	3	0.326(21)	-1.69(4.03)	1.17

Table 3.6: Table of our fitting values of $\alpha_s(m_\tau^2)$, and c_8 for the single pinched fourth power monomial weight $\omega(x) = 1-x^3$ using FOPT ordered by increasing s_{min}. The errors are given in parenthesis after the observed value.

3.7.5 Single pinched fourth power monomial: $\omega(x) = 1 - x^4$

s_{min}	$\#s_0$s	$\alpha_s(m_\tau^2)$	c_{10}	χ^2/dof
1.500	23	0.3144(27)	-0.572(80)	2.44
1.525	22	0.3155(27)	-0.655(90)	2.34
1.550	21	0.3157(28)	-0.671(99)	2.45
1.575	20	0.3171(28)	-0.80(11)	2.1
1.600	19	0.3173(29)	-0.82(12)	2.21
1.625	18	0.3180(29)	-0.88(13)	2.24
1.650	17	0.3190(30)	-0.98(14)	2.1
1.675	16	0.3189(30)	-0.97(15)	2.24
1.700	15	0.3192(30)	-1.00(16)	2.39
1.750	14	0.3188(32)	-0.96(19)	2.58
1.800	13	0.3204(32)	-1.17(21)	2.39
1.850	12	0.3190(34)	-0.95(26)	2.4
1.900	11	0.3189(35)	-0.94(29)	2.67
1.950	10	0.3149(37)	-0.31(34)	1.47
2.000	9	0.3137(39)	-0.08(39)	1.5
2.100	8	0.3136(43)	-0.07(54)	1.75
2.200	7	0.3203(48)	-1.64(77)	0.42
2.300	6	0.3216(56)	-2.01(1.13)	0.47
2.400	5	0.3247(66)	-2.98(1.62)	0.39
2.600	4	0.324(10)	-2.86(3.69)	0.58
2.800	3	0.325(20)	-3.43(10.74)	1.17

Table 3.7: Table of our fitting values of $\alpha_s(m_\tau^2)$ and c_{10} for the single pinched fourth power monomial weight $\omega(x) = 1 - x^4$ using FOPT ordered by increasing s_{min}. The errors are given in parenthesis after the observed value.

3.7.6 Optimal Moments

$$\omega^{(n,m)}(x) = (1-x)^n \sum_{k=0}^{m} (k+1)x^k \tag{3.67}$$

$\omega(x) = (1-x)^2$

s_{min}	$\#s_0$s	$\alpha_s(m_\tau^2)$	$aGGInv$	c_6	χ^2/dof
1.500	23	0.3276(13)	-0.0077(10)	0.330(35)	2.62
1.525	22	0.3278(14)	-0.0078(10)	0.330(38)	2.75
1.550	21	0.3299(16)	-0.0092(12)	0.333(37)	2.31
1.575	20	0.3308(25)	-0.0098(13)	0.334(47)	2.32
1.600	19	0.3317(28)	-0.0105(14)	0.335(54)	2.38
1.625	18	0.3336(21)	-0.0118(14)	0.340(46)	2.09
1.650	17	0.3345(34)	-0.0124(17)	0.342(62)	2.15
1.675	16	0.3349(25)	-0.0127(15)	0.342(51)	2.28
1.700	15	0.3348(33)	-0.0126(18)	0.342(58)	2.47
1.750	14	0.3372(43)	-0.0145(23)	0.341(71)	2.34
1.800	13	0.3378(31)	-0.0149(20)	0.339(58)	2.54
1.850	12	0.3365(38)	-0.0138(25)	0.346(60)	2.72
1.900	11	0.3355(40)	-0.0128(28)	0.354(59)	2.97
1.950	10	0.3296(47)	-0.0073(34)	0.418(58)	1.57
2.000	9	0.3299(50)	-0.0076(39)	0.414(64)	1.83
2.100	8	0.3331(54)	-0.0108(45)	0.361(76)	1.9
2.200	7	0.3401(57)	-0.0185(52)	0.220(88)	0.73
2.300	6	0.3383(68)	-0.0165(67)	0.26(12)	0.89
2.400	5	0.3450(93)	-0.0243(99)	0.10(17)	0.71
2.600	4	0.337(16)	-0.014(18)	0.36(45)	0.98

Table 3.8: Table of our fitting values of $\alpha_s(m_\tau^2), aGGInv$ and c_6 for the triple pinched optimal weight $\omega^{(2,0)}(x) = (1-x)^2$ using FOPT ordered by increasing s_{min}. The errors are given in parenthesis after the observed value.

$\omega(x) = (1-x)^3$

s_{min}	$\#s_0$s	$\alpha_s(m_\tau^2)$	$aGGInv$	c_6	c_8	χ^2/dof
1.900	11	0.34281(92)	-0.01473(73)	-0.103(22)	-0.534(46)	1.52
1.950	10	0.34154(99)	-0.01304(61)	-0.050(17)	-0.389(44)	1.42
2.000	9	0.33985(81)	-0.01124(43)	0.002(10)	-0.242(26)	1.59
2.100	8	0.3480(47)	-0.0201(36)	-0.264(89)	-1.03(28)	0.31
2.200	7	0.3483(23)	-0.0204(41)	-0.27(15)	-1.05(40)	0.41
2.300	6	0.3522(64)	-0.0249(62)	-0.42(18)	-1.51(57)	0.29
2.400	5	0.3480(89)	-0.0199(100)	-0.25(33)	-0.96(10)	0.39

Table 3.9: Table of our fitting values of $\alpha_s(m_\tau^2), aGGInv, c_6$ and c_8 for the optimal weight $\omega^{(3,0)}(x) = (1-x)^3$ using FOPT ordered by increasing s_{min}. The errors are given in parenthesis after the observed value.

3.7.7 Comparison

weight	$\alpha_s(m_\tau^2)$	c_6	c_8	χ^2/dof
$\omega_{kin}^{(D6,D8)}$	0.3232(32)	-0.31(11)	-0.01(18)	1.13
$\omega_{cube}^{(D6,D8)}$	0.3261(21)	-0.309(27)	-0.136(18)	1.17
$\omega_{cube}^{(D6,D8,D10)}$	0.3312(43)	-0.56(12)	-0.68(23)	1.17
$\omega_{quartic}^{(D6,D8)}$	0.3266(27)	-0.235(28)	-0.087(17)	1.0
$\omega_{quartic}^{(D6,D8,D10)}$	0.3308(12)	-0.3499(62)	-0.2453(55)	1.21
$\omega_{quartic}^{(D6,D8,D10,D12)}$	0.3290(11)	-0.3030(46)	-0.1874(28)	0.67
$\omega_{monoX3}^{(D8)}$	0.326(21)	-	-1.69(40)	1.17
$\omega_{monoX4}^{(D10)}$	0.325(20)	-	-	1.17
$\omega_{opt20}^{(D4,D6)}$	0.337(16)	0.36(45)	-	0.98
$\omega_{opt30}^{(D4,D6,D8)}$	0.34154(99)	-0.050(17)	-0.389(44)	1.42

Table 3.10: Table of the best fits (selected by χ^2/dof closest to one) for each weight including the strong coupling $\alpha_s(m_\tau^2)$ as a fitting variable.

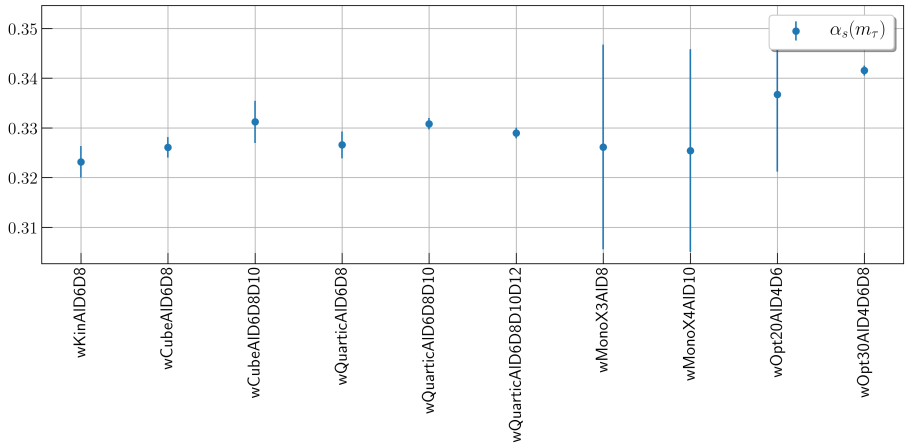

Figure 3.7: Comparison of the strong coupling for the best fits (selected by χ^2/dof closest to one) for each weight including the strong coupling as a fitting variable.

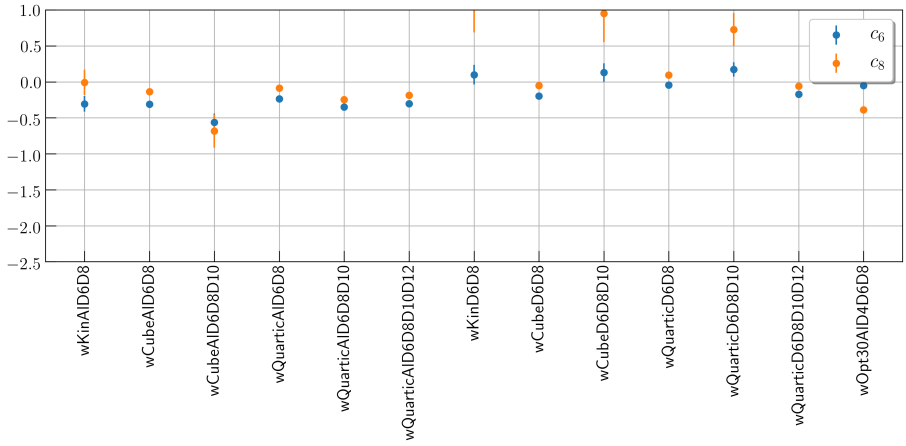

Figure 3.8: Comparison of the dimension six and eight values for the best fits (selected by χ^2/dof closest to one) for each weight including the OPE dimensions six and eight as fitting variables.

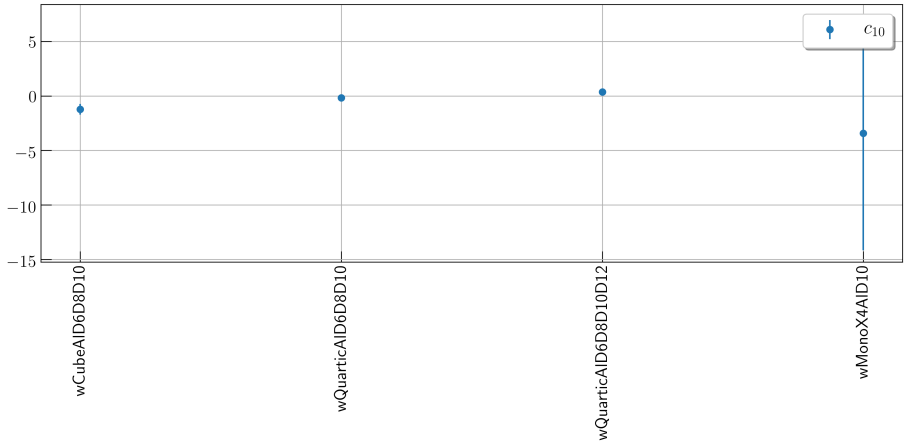

Figure 3.9: Comparison of the dimension ten values for the best fits (selected by χ^2/dof closest to one) for each weight including the OPE dimensions ten as fitting variables.

3.7.8 Toni Pich 2006

4. ALEPH determination

Toni built moments with five different weights:

$$\omega_{kl(x)} = (1-x)^{2+k}x^l(1+x) \quad \text{with} \quad (k,l) = (0,0),(1,0),(1,1),(1,2),(1,3) \tag{3.68}$$

He always fitted weight combinations, which we do not include.

5. Optimal moments

Used single moments

$$\omega^{(n,m)}(x) = (1-x)^n \sum_{k=0}^{n}(k+1)x^k \quad \text{with} \quad (n,m) = (1,0),(1,1),(1,2),(1,3),(1,4),(1,5),(2,0),(2,1),(2,2),(2,3) \tag{3.69}$$

but omitted NPT corrections! He fitted the kinematic weight with free α_s for $\omega(x)^{(2,1)}$. Later on he uses combined fits which is not in our interest. It is called optimal moments, because n stands for the pinching factor, which suppresses DV!

6. Including information from the s_0 dependence

Pich fits $A^{(2,0)}, A^{(2,1)}$ and $A^{(2,2)}$ separately for $s_{min} = 2\,\text{GeV}$. The corresponding weights with fitted OPE dimensions are given by:

$$\omega^{(2,0)} = (1-x)^2 \quad c_4, c_6 \tag{3.70}$$

$$\omega^{(2,1)} = \omega_\tau \quad c_6, c_8 \tag{3.71}$$

$$\omega^{(2,2)} = (1-x)^2(1+2x+x^2) = (x^2-1)^2 \quad c_8, c_{10} \tag{3.72}$$

Thus we can compare our results from the kinematic weight with his results and furthermore add $(1-x)^2$ to our fitting list?

Alpha is comparable, which just have a bigger error. For D6 and D8 we have to compare our definition of c_6, c_8 with his.

Chapter 4

Derivation of the used inverse covariance matrix from the Aleph data

While performing a **Generalized least squares** (GLS) we estimate our regression coefficients $\hat{\beta}$ as follows:

$$\hat{\beta} = \underset{b}{\operatorname{argmin}}(\mathbf{y} - \mathbf{Xb})^{\intercal}\mathbf{\Omega}^{-1}(\mathbf{y} - \mathbf{Xb}), \tag{4.1}$$

with $\mathbf{b}$ being an candidate estimate of β, $\mathbf{X}$ being the design matrix, $\mathbf{y}$ being the response values and $\mathbf{\Omega}^{-1}$ being the **inverse covariance matrix**.

The Aleph data includes the **standard error** (SE), which are equal to the **standard deviation** as per definition. Furthermore Aleph provides the **correlation coefficients** of the errors. We will use these two quantities in combination with **Gaussian error propagation** to derive derive an approximation of the covariance matrix.

4.1 Propagation of experimental errors and correlation

Let $\{f_k(x_1, x_2, \cdots x_n)\}$ be a set of m functions, which a linear combinations of n variables $x_1, x_2, \cdots x_n$ with combination coefficients $A_{k1}, A_{k2}, \cdots A_{kn}$, where $k \in \{1, 2, \cdots, m\}$. Let the covariance matrix of x_n be denoted by

$$\Sigma^x = \begin{pmatrix} \sigma_1^2 & \sigma_{12} & \sigma_{13} & \cdots \\ \sigma_{12} & \sigma_2^2 & \sigma_{23} & \cdots \\ \sigma_{13} & \sigma_{23} & \sigma_3^2 & \cdots \\ \vdots & \vdots & \vdots & \ddots \end{pmatrix}. \tag{4.2}$$

Then the covariance matrix of the functions Σ^f is given by

$$\Sigma^f_{ij} = \sum_k^n \sum_l^n A_{ik} \sum_{kl}^x A_{jl}, \quad \Sigma^f = A\Sigma^x A^\intercal. \tag{4.3}$$

In our case we are dealing with non-linear functions, which we will linearized with the help of the **Taylor expansion**

$$f_k \approx f_k^0 + \sum_i^n \frac{\partial f_k}{\partial x_i} x_i, \quad f \approx f^0 + Jx. \tag{4.4}$$

Therefore, the propagation of error follows from the linear case, replacing the Jacobian matrix with the combination coefficients ($J = A$)

Chapter 5

Coefficients

5.1 β function

There are several conventions for defining the β coefficients, depending on a minus sign and/or a factor of two (if one substitues $\mu \to \mu^2$) in the β-function 2.5. We follow the convention from Pascual and Tarrach (except for the minus sign) and have taken the values from [3]

$$\beta_1 = \frac{1}{6}(11N_c - 2N_f) \tag{5.1}$$

$$\beta_2 = \frac{1}{12}(17N_c^2 - 5N_cN_f - 3C_fN_f) \tag{5.2}$$

$$\beta_3 = \frac{1}{32}\left(\frac{2857}{54}N_c^3 - \frac{1415}{54}N_c^2N_f + \frac{79}{54}N_cN_f^2 - \frac{205}{18}N_cC_fN_f + \frac{11}{9}C_fN_f^2 + C_f^2N_f\right) \tag{5.3}$$

$$\beta_4 = \frac{140599}{2304} + \frac{445}{16}\zeta_3, \tag{5.4}$$

where we used $N_f = 6$ and $N_c = 3$ for β_4.

5.2 Anomalous mass dimension

5.3 Adler function

Bibliography

[1] P. A. Baikov, K. G. Chetyrkin, and Johann H. Kuhn. "Order alpha**4(s) QCD Corrections to Z and tau Decays". In: *Phys. Rev. Lett.* 101 (2008), p. 012002. DOI: 10.1103/PhysRevLett.101.012002. arXiv: 0801.1821 [hep-ph].

[2] Martin Beneke and Matthias Jamin. "alpha(s) and the tau hadronic width: fixed-order, contour-improved and higher-order perturbation theory". In: *JHEP* 09 (2008), p. 044. DOI: 10.1088/1126-6708/2008/09/044. arXiv: 0806.3156 [hep-ph].

[3] Diogo Boito et al. "A new determination of $\alpha_s from hadronic \tau decays$". In: *Phys. Rev.* D84 (2011), p. 113006. DOI: 10.1103/PhysRevD.84.113006. arXiv: 1110.1127 [hep-ph].

[4] Diogo Boito et al. "Strong coupling from e^+e^- → hadrons below charm". In: *Phys. Rev.* D98.7 (2018), p. 074030. DOI: 10.1103/PhysRevD.98.074030. arXiv: 1805.08176 [hep-ph].

[5] Diogo Boito et al. "Strong coupling from the revised ALEPH data for hadronic τ decays". In: *Phys. Rev.* D91.3 (2015), p. 034003. DOI: 10.1103/PhysRevD.91.034003. arXiv: 1410.3528 [hep-ph].

[6] E. Braaten, Stephan Narison, and A. Pich. "QCD analysis of the tau hadronic width". In: *Nucl. Phys.* B373 (1992), pp. 581–612. DOI: 10.1016/0550-3213(92)90267-F.

[7] David J. Broadhurst. "Chiral Symmetry Breaking and Perturbative QCD". In: *Phys. Lett.* 101B (1981), pp. 423–426. DOI: 10.1016/0370-2693(81)90167-2.

[8] Irinel Caprini and Jan Fischer. "alpha(s) from tau decays: Contour-improved versus fixed-order summation in a new QCD perturbation expansion". In: *Eur. Phys. J.* C64 (2009), pp. 35–45. DOI: 10.1140/epjc/s10052-009-1142-8. arXiv: 0906.5211 [hep-ph].

[9] Oscar Cata, Maarten Golterman, and Santi Peris. "Unraveling duality violations in hadronic tau decays". In: *Phys. Rev.* D77 (2008), p. 093006. DOI: 10.1103/PhysRevD.77.093006. arXiv: 0803.0246 [hep-ph].

[10] William Celmaster and Richard J. Gonsalves. "An Analytic Calculation of Higher Order Quantum Chromodynamic Corrections in e+ e- Annihilation". In: *Phys. Rev. Lett.* 44 (1980), p. 560. DOI: 10.1103/PhysRevLett.44.560.

[11] K. G. Chetyrkin, A. L. Kataev, and F. V. Tkachov. "Higher Order Corrections to Sigma-t (e+ e- —¿ Hadrons) in Quantum Chromodynamics". In: *Phys. Lett.* 85B (1979), pp. 277–279. DOI: 10.1016/0370-2693(79)90596-3.

[12] M. Davier et al. "The Determination of alpha(s) from Tau Decays Revisited". In: *Eur. Phys. J.* C56 (2008), pp. 305–322. DOI: 10.1140/epjc/s10052-008-0666-7. arXiv: 0803.0979 [hep-ph].

[13] Michel Davier, Andreas Hocker, and Zhiqing Zhang. "ALEPH Tau Spectral Functions and QCD". In: *Nucl. Phys. Proc. Suppl.* 169 (2007). [,22(2007)], pp. 22–35. DOI: 10.1016/j.nuclphysbps.2007.02.109. arXiv: hep-ph/0701170 [hep-ph].

[14] Michel Davier, Andreas Höcker, and Zhiqing Zhang. "The physics of hadronic tau decays". In: *Rev. Mod. Phys.* 78 (4 Oct. 2006), pp. 1043–1109. DOI: 10.1103/RevModPhys.78.1043. URL: https://link.aps.org/doi/10.1103/RevModPhys.78.1043.

[15] Michel Davier et al. "Update of the ALEPH non-strange spectral functions from hadronic τ decays". In: *Eur. Phys. J.* C74.3 (2014), p. 2803. DOI: 10.1140/epjc/s10052-014-2803-9. arXiv: 1312.1501 [hep-ex].

[16] Michael Dine and J. R. Sapirstein. "Higher Order QCD Corrections in e+ e- Annihilation". In: *Phys. Rev. Lett.* 43 (1979), p. 668. DOI: 10.1103/PhysRevLett.43.668.

[17] S. G. Gorishnii, A. L. Kataev, and S. A. Larin. "The $O(\alpha_s^3)$-corrections to $\sigma_{tot}(e^+e^- \to hadrons)$ and $\Gamma(\tau^- \to \nu_\tau + hadrons)$ in QCD". In: *Phys. Lett.* B259 (1991), pp. 144–150. DOI: 10.1016/0370-2693(91)90149-K.

[18] Matthias Jamin. "Contour-improved versus fixed-order perturbation theory in hadronic tau decays". In: *JHEP* 09 (2005), p. 058. DOI: 10.1088/1126-6708/2005/09/058. arXiv: hep-ph/0509001 [hep-ph].

[19] Matthias Jamin. *QCD and Renormalisation Group Methods.* Lecture presented at Herbstschule für Hochenergiephysik Maria Laach. Sept. 2006.

[20] Matthias Jamin and Manfred Munz. "Current correlators to all orders in the quark masses". In: *Z. Phys.* C60 (1993), pp. 569–578. DOI: 10.1007/BF01560056. arXiv: hep-ph/9208201 [hep-ph].

[21] Gunnar Kallen. "On the definition of the Renormalization Constants in Quantum Electrodynamics". In: *Helv. Phys. Acta* 25 (417). [,509(1952)]. DOI: 10.1007/978-3-319-00627-7_90.

[22] Alexander Keshavarzi, Daisuke Nomura, and Thomas Teubner. "Muon $g-2$ and $\alpha(M_Z^2)$: a new data-based analysis". In: *Phys. Rev.* D97.11 (2018), p. 114025. DOI: 10.1103/PhysRevD.97.114025. arXiv: 1802.02995 [hep-ph].

[23] L. V. Lanin, V. P. Spiridonov, and K. G. Chetyrkin. "Contribution of Four Quark Condensates to Sum Rules for ρ and A1 Mesons. (In Russian)". In: *Yad. Fiz.* 44 (1986), pp. 1372–1374.

[24] H. Lehmann. "On the Properties of propagation functions and renormalization contants of quantized fields". In: *Nuovo Cim.* 11 (1954), pp. 342–357. DOI: 10.1007/BF02783624.

[25] R. Tarrach P. Pascual. *QCD: Renormalization for the Practitioner*. Springer-Verlag, 1984.

[26] Michael E. Peskin and Daniel V. Schroeder. *An Introduction to quantum field theory*. Reading, USA: Addison-Wesley, 1995. URL: http://www.slac.stanford.edu/~mpeskin/QFT.html.

[27] Antonio Pich. "Precision Tau Physics". In: *Prog. Part. Nucl. Phys.* 75 (2014), pp. 41–85. DOI: 10.1016/j.ppnp.2013.11.002. arXiv: 1310.7922 [hep-ph].

[28] Antonio Pich and Antonio Rodríguez-Sánchez. "Determination of the QCD coupling from ALEPH τ decay data". In: *Phys. Rev. D* 94 (3 Aug. 2016), p. 034027. DOI: 10.1103/PhysRevD.94.034027. URL: https://link.aps.org/doi/10.1103/PhysRevD.94.034027.

[29] Eduardo de Rafael. "An Introduction to sum rules in QCD: Course". In: *Probing the standard model of particle interactions. Proceedings, Summer School in Theoretical Physics, NATO Advanced Study Institute, 68th session, Les Houches, France, July 28-September 5, 1997. Pt. 1, 2.* 1997, pp. 1171–1218. arXiv: hep-ph/9802448 [hep-ph].

[30] S. Schael et al. "Branching ratios and spectral functions of tau decays: Final ALEPH measurements and physics implications". In: *Phys. Rept.* 421 (2005), pp. 191–284. DOI: 10.1016/j.physrep.2005.06.007. arXiv: hep-ex/0506072 [hep-ex].

[31] Felix Schwab. "Strange Quark Mass Determination From Sum Rules For Hadronic τ-Decays". German. MA thesis. somewhere, 2002.

[32] Mikhail A. Shifman, A. I. Vainshtein, and Valentin I. Zakharov. "QCD and Resonance Physics: Applications". In: *Nucl. Phys.* B147 (1979), pp. 448–518. DOI: 10.1016/0550-3213(79)90023-3.

[33] Mikhail A. Shifman, A. I. Vainshtein, and Valentin I. Zakharov. "QCD and Resonance Physics. Theoretical Foundations". In: *Nucl. Phys.* B147 (1979), pp. 385–447. DOI: 10.1016/0550-3213(79)90022-1.

[34] Levan R. Surguladze and Mark A. Samuel. "Total hadronic cross-section in e+ e- annihilation at the four loop level of perturbative QCD". In: *Phys. Rev. Lett.* 66 (1991). [Erratum: Phys. Rev. Lett.66,2416(1991)], pp. 560–563.

[35] M. Tanabashi et al. "Review of Particle Physics". In: *Phys. Rev.* D98.3 (2018), p. 030001. DOI: 10.1103/PhysRevD.98.030001.

[36] Yung-Su Tsai. "Decay Correlations of Heavy Leptons in $e^+ + e^- \to l^+ + l^-$". In: *Phys. Rev. D* 4 (9 Nov. 1971), pp. 2821–2837. DOI: 10.1103/PhysRevD.4.2821. URL: https://link.aps.org/doi/10.1103/PhysRevD.4.2821.

[37] Steven Weinberg. "Phenomenological Lagrangians". In: *Physica* A96.1-2 (1979), pp. 327–340. DOI: 10.1016/0378-4371(79)90223-1.

[38] Kenneth G. Wilson. "Confinement of quarks". In: *Phys. Rev. D* 10 (8 Oct. 1974), pp. 2445–2459. DOI: 10.1103/PhysRevD.10.2445. URL: https://link.aps.org/doi/10.1103/PhysRevD.10.2445.

[39] Kenneth G. Wilson. "Nonlagrangian models of current algebra". In: *Phys. Rev.* 179 (1969), pp. 1499–1512. DOI: 10.1103/PhysRev.179.1499.